

DEPLOYMENT AND COVERAGE MAINTENANCE
IN MOBILE SENSOR NETWORKS

A Dissertation

by

JAEYONG LEE

Submitted to the Office of Graduate Studies of
Texas A&M University
in partial fulfillment of the requirements for the degree of

DOCTOR OF PHILOSOPHY

August 2007

Major Subject: Mechanical Engineering

DEPLOYMENT AND COVERAGE MAINTENANCE
IN MOBILE SENSOR NETWORKS

A Dissertation

by

JAEYONG LEE

Submitted to the Office of Graduate Studies of
Texas A&M University
in partial fulfillment of the requirements for the degree of

DOCTOR OF PHILOSOPHY

Approved by:

Chair of Committee,	Suhada Jayasuriya
Committee Members,	Alexander Parlos
	Won-jong Kim
	Jennifer L. Welch
Head of Department,	Dennis O'Neal

August 2007

Major Subject: Electrical Engineering

ABSTRACT

Deployment and Coverage Maintenance
in Mobile Sensor Networks . (August 2007)

Jaeyong Lee, B.S., Pusan National University, Busan, Korea;
M.S., Texas A&M University.

Chair of Advisory Committee: Dr. Suhada Jayasuriya

Deployment of mobile nodes in a region of interest is a critical issue in building a mobile sensor network because it affects cost and detection capabilities of the system. The deployment of mobile sensors in essence is the movement of sensors from an initial position to a final optimal location. Considerable attention has recently been given to this deployment issue. Many of the distributed deployment schemes use the potential field method. In most cases, the negative gradient of the potential function becomes the feedback control input to a node. This assumes that the potential function is differentiable over the entire region. This assumption is valid primarily when the topology of the network is fixed.

In this research, we analyze the stability of a network that uses piecewise smooth potential functions. A gravitation-like force is proposed to deploy a group of agents and to form a certain configuration. We use a nonsmooth version of the Lyapunov stability theory and LaSalle's invariance principle to show asymptotic stability of the network which is governed by discontinuous dynamics.

We propose a hierarchical structure using potential fields for mobile sensor network deployment. A group of mobile nodes first form a cluster using a potential field method and then cluster heads are used to establish a hexagonal structure that employs a higher level potential field.

We consider specifically the problem of deploying a mobile sensor network so that a certain area coverage is realized and maintained. And we propose an algorithm for main-

taining the desired coverage that assumes the availability of a stochastic sensor model. The model reflects the decline of the sensor accuracy as the distance increases from the sensor. It is further assumed that each node's sensor has a different sensing range to represent sensor performance deterioration due to power decay. The network deployment scheme combines artificial forces with individual sensor ranges. The validity and the effectiveness of the proposed algorithm are compared to the conventional methods in simulations. Simulation results confirm the effectiveness of the proposed algorithms with respect to a defined performance metric.

To my father and mother,
who have always given me love and support,

To my daughters,
who have always made me happy,

and To my wife, Seojung,
who has devoted her life to supporting me

ACKNOWLEDGMENTS

First of all, I would like to thank my advisor, Dr. Suhada Jayasuriya, for his consistent guidance and support during my Ph.D. course. Without his insightful guidance, this work would have not been possible. I would also like to thank committee members, Dr. Alexander Parlos, Dr. Won-jong Kim, and Dr. Jennifer Welch, for their helpful advise and comments on my work.

My father and mother sacrificed much to provide me opportunities to have a good education and they encouraged me so that I could choose what I wanted to be and to do. I would like to show my love and thanks for what they have done for me throughout my life.

I also wish to thank all the colleagues in the Center for Dynamic Systems and Control. Discussion with them was always hilarious, and their help is so much appreciated.

Last, but not least, I would like to thank my wife, Seojung Kim, for her support, encouragement, and unlimited belief in me.

TABLE OF CONTENTS

CHAPTER		Page
I	INTRODUCTION	1
	A. Mobile Sensor Networks	1
	B. Sensor Network Coverage and Deployment	2
	C. Contributions	4
	D. Dissertation Structure	5
II	SENSOR NETWORK DEPLOYMENT AND STABILITY ANALYSIS OF TIME INVARIANT SYSTEM	6
	A. Definitions	6
	B. Network Deployment	7
	1. Hexagonal deployment	9
	C. Stability Analysis for Time Invariant System	12
III	STABILITY ANALYSIS FOR DISCONTINUOUS DYNAMIC SYSTEM	15
	A. Preliminaries	15
	1. Piecewise smooth vector field	15
	2. Lyapunov stability of nonsmooth systems	16
	B. Discontinuous Dynamic Systems	19
IV	HIERARCHICAL NETWORK DEPLOYMENT	26
	A. Clustering in Mobile Sensor Networks	26
	1. Clustering scheme	26
	B. Active Nodes and Passive Nodes	28
	1. Definitions	28
	2. Stability analysis	30
	3. Forming clusters and merging	32
	C. Simulation Results	32
	1. Hexagonal structure formation	33
	2. Hierarchical application for deployment	34
V	COVERAGE MAINTENANCE FOR TIME VARYING SYSTEM	38
	A. Coverage Maintenance	38

CHAPTER	Page
1. Stochastic sensor model	38
2. Unequal sensor ranges	43
3. Time varying system	45
B. Simulation Results	46
VI HARDWARE DEVELOPMENT	53
A. Mobile Base	53
B. Mobile Robot Control System	54
C. Communication Part	54
1. Wireless module	54
2. Voltage coverter	55
D. Motor Control Part	56
1. Controller	56
2. Interrupt	57
3. Motor speed control	58
4. Mapping artificial force to a real robot	58
VII CONCLUSIONS AND FUTURE WORK	60
A. Summary and Conclusions	60
B. Directions for Future Research	63
REFERENCES	65
VITA	69

LIST OF TABLES

TABLE		Page
I	Components of a mobile robot for communication and motor control . . .	55
II	Communication unit (MCB3100) specifications	55
III	Pin connection of MCB3100	56

LIST OF FIGURES

FIGURE		Page
1	Sensor model and coverage	8
2	Optimal placement using disk packing problem	9
3	Force model and hexagonal structure	10
4	Undirected graph and its spacial representation	13
5	Piecewise smooth vector field	16
6	Force model	20
7	Potential energy derived from the force law	22
8	Concept of active and passive nodes	28
9	Mixed (directed and undirected) graph	29
10	Clusters and merging	31
11	Hexagonal structure construction	33
12	Effect of different values of α	34
13	Deployment sequence	36
14	Performance comparison between the incremental and hierarchical algorithms in terms of uniformity	37
15	Sensor models	39
16	Cumulative probability distributions	41
17	Nonhomogeneous sensor ranges	44
18	4 sensor nodes with 2 different ranges	45

FIGURE	Page
19	Changes in sensor performance due to r_e 46
20	Mobile sensor unit with power alert 46
21	Initial deployment of the mobile nodes 48
22	Sensing range deterioration due to the power drainage 49
23	Coverage maintenance with constant d 50
24	Coverage maintenance with time varying d 51
25	Fraction of the covered area for two cases 52
26	Mobile robot base: Rex-12 from Zagros Robotics 53
27	System diagram for a mobile robot with power and information flows . . . 54
28	Physical connection between the modules 56
29	Max232 pin connections 57

CHAPTER I

INTRODUCTION

A. Mobile Sensor Networks

Recent achievements in wireless communications and electronic technologies have enabled the development of sensor nodes in a network topology which can provide access to information anytime, anywhere by collecting, processing, analyzing and disseminating data. Networking these sensor nodes and providing them an ability to coordinate amongst themselves for larger sensing tasks can revolutionize information gathering and processing in many situations.

This revolutionary sensor network technology has given a lot of advantages in performance, flexibility, robustness, and functionality for sensor-oriented tasks such as environment monitoring [1], fire detection [2], and other complex monitoring tasks [3]. With the advances in technologies, the usefulness of sensor network has stimulated more applications in unpredictable, previously unknown, and even hostile environments.

A mobile sensor network comprises of a distributed collection of nodes, each of which has sensing, computation, communication and locomotion capabilities. It is this latter capability that distinguishes a mobile sensor network from a conventional static network. Locomotion facilitates a number of useful network capabilities, including the ability to self-deploy; that is, starting from some compact initial configuration, the nodes in a network can propagate by spreading out such that the area covered by the network is maximized. Due to the inextricable relation to the physical world, the proper deployment of sensors is very important for a successful completion of sensing tasks.

Self deployment methods using mobile nodes have been proposed to enhance net-

The journal model is *IEEE Transactions on Automatic Control*.

work coverage and to extend the system lifetime by configuring uniformly distributed node topologies from random node distributions. Since mobility itself requires energy from its own limited energy sources, a deployment scheme should be designed carefully to minimize energy consumption during deployment, while achieving certain goals, such as satisfactory coverage and an energy-efficient node topology.

B. Sensor Network Coverage and Deployment

The sensor location problem in mobile sensor networks has similarities to the conventional art gallery problem (AGP) studied in computational geometry [4]. AGP seeks to determine how to use a minimal number of guards (cameras) in a polygon so that every point in the polygon is observed by at least one guard (camera). However, the solutions of AGP cannot be directly applied to the mobile sensor network deployment problem. First, AGP solutions assume that the model of an environment can be well constructed *a priori*. This is not typical in mobile sensor network deployment. Secondly, AGP solutions suppose that a guard can observe as long as a line-of-sight exists, while sensors usually have finite sensing ranges. Furthermore, AGP solutions do not consider the limitations imposed by communication range.

The problems of coverage and deployment are fundamentally interrelated. In [5], the authors have discussed the problem of location and deployment of sensors from a coverage standpoint. The authors define the coverage problem from different points of view, including deterministic, statistical, and the worst and best cases. The goal is to have each location in the environment covered by at least one sensor. They argue that coverage is a primary performance metric that determines quality-of-service (QoS) and combined computational geometry and graph theory for their algorithms.

The concept of coverage as a paradigm for the system-level functionality of multi-

robot systems was introduced by Gage [6]. Gage defines three basic types of coverage: (i) Blanket, (ii) Barrier, and (iii) Sweep coverage. In *Blanket coverage*, the objective is to accomplish a static arrangement of nodes that maximizes the total detection area. The objective of *Barrier coverage* is to minimize the probability of undetected penetration through the barrier. *Sweep coverage* is roughly equivalent to the moving *Barrier coverage*. According to this taxonomy, the deployment problem in this research is equivalent to blanket coverage.

Autonomous mobile sensor deployment algorithms have been intensively researched. One of the most widely used methods is to employ artificial force concept between mobile agents. Since first presented by Khatib [7], potential field based methods have been extensively used in path planning. In potential field based algorithms [8] [9] [10], a control law is defined as the negative gradient of the potential. Popa *et al.* [11] deployed sensor networks using conventional potential field method. Voronoi diagram method has also been used to generate artificial forces [12]. On applying these algorithms, the mobile sensor nodes get situated in the environment in a distributed manner. A Virtual force can be directly derived to enhance network coverage for randomly placed sensors as developed by [13].

Most of the previous research, however, assumed a smooth potential field which is differentiable over the entire region. This assumes two properties. First assumption is that a neighboring set (a set of nodes with which a node can communicate) of a node never changes, and the second is that a potential function is differentiable. A force field derived from a smooth potential function becomes continuous, and the system is governed by continuous dynamics.

We remove the second assumption on the continuity of a force field. We develop a system represented by differential equations with discontinuous right hand side, where interactive forces between nodes are discontinuous. We followed the framework by Shenvitz and Paden [14] to prove stability. The main advantage of this work is to grant much

freedom in designing a force field or shaping a potential field for a network formation.

C. Contributions

The main goals of this dissertation are to prove stability of the system which uses an artificial force derived from potential functions, and to develop algorithms which improve the system performance. The proposed research was aimed at achieving goals by completing the following objectives.

1. To develop a force model which achieve optimal placement.
2. To analyze stability of the system which has discontinuous right hand side in its differential equation characterization.
3. To develop a deployment strategy which uses a hierarchial structure to achieve better coverage.
4. To implement a heterogeneous sensor model to maintain better coverage compared to a homogeneous sensor model.
5. To develop and fabricate multi purpose mobile sensor base to implement our algorithms.

Our approach to achieve desirable deployment is to use potential fields which generate artificial forces. We show that a hexagonal structure formation guarantees maximal coverage area as per our terminology. Each node is fundamentally controlled by an artificial force derived from a conventional potential field. We begin to construct the network by distributing mobile nodes into a region of interest. The nodes deploy by interacting with nearby sensor nodes. A hierarchical approach to achieve this hexagonal structure for a wider area is developed without any additional complicated algorithms.

In conventional artificial force algorithms, the sensors are placed so that they keep predefined distances between them. We implement a stochastic sensor model that redefines

the distance to be maintained by the sensor nodes. We incorporate mobile sensor network deployment and coverage maintenance by combining potential field based artificial forces and stochastic sensor models. Power status of a sensor is reflected in the selection of this sensor model so that the network can maintain the desired sensing performance. Compared to current power level, each node determines a valid sensing range, and by exchanging this information with a neighbor, a new optimal distance is derived. This distance information is in turn used to generate the artificial force between two nodes.

D. Dissertation Structure

The remainder of this dissertation is organized as follows.

In chapter II, explained are the general terminologies used in this dissertation, and a network deployment algorithm using the conventional potential field formalism. Mobile nodes are deployed by artificial forces derived from potential functions. Chapter III focusses on the stability issues of the system described by differential equations with discontinues right hand side. Chapter IV is concerned with the network deployment and a hierarchical coverage control algorithm. In chapter V, explained is the coverage maintenance method which enhances overall detection probability by using a time varying sensor model. Chapter VII concludes this dissertation by summarizing our works and presenting issues for future research.

CHAPTER II

SENSOR NETWORK DEPLOYMENT AND STABILITY ANALYSIS OF TIME
INVARIANT SYSTEM

The stability of the time invariant system is analyzed with conventional Lyapunov theory.

A. Definitions

Definition A.1 *Let us suppose that a sensor s is located at (x_s, y_s) and it has sensing range r . We assume that a sensor has disk type sensing range. Then a point p is said to be covered by a sensor s if $\text{dist}(s, p) \leq r$.*

Definition A.2 *For the given region of interest A_i , the coverage of a sensor network is the area A_c within which every point p is covered by at least one sensor.*

Definition A.3 *A vector field on R^n is a mapping*

$$f : X \subseteq R^n \rightarrow R^n. \quad (2.1)$$

A vector field assigns to each point x in X a vector $f(x)$ in R^n , represented by an arrow whose tail is at the point x .

Definition A.4 *A gradient field on R^n is a vector field*

$$f : X \subseteq R^n \rightarrow R^n \quad (2.2)$$

such that f is the gradient of some (differentiable) scalar-valued function

$$V : X \rightarrow R. \quad (2.3)$$

That is $f(x) = \nabla V(x)$, at all x in X . The function V is called a (scalar) potential function for the vector field f .

B. Network Deployment

An important phase in the operation of a sensor network is the deployment of sensors in a field of interest. It is a critical issue because it directly affects the cost and detection capability of a wireless sensor network. Sensor deployment has received considerable attention recently. Critical goals during deployment of a sensor network include coverage, connectivity, and load balancing among others.

The deployment strategy for sensor networks varies with the application considered. It can be predetermined when the environment is sufficiently known and under control, in which case the sensors can be strategically deployed manually.

The deployment can also be *a priori* undetermined when the environment is unknown or hostile, such as remote harsh fields, disaster areas and toxic urban regions. In this case, sensor deployment cannot be pre-planned and performed manually. For example, the sensors may be airdropped from an aircraft or deployed by other means, generally resulting in a random placement. Random placement of sensors in a target area is often desirable especially if no *a priori* knowledge of the terrain is available. Random deployment is practical in military applications, where sensor networks are initially established by dropping or throwing sensors into a desired field. However, such random deployment does not always lead to effective coverage, especially if the sensors are overly clustered and there is a small concentration of sensors in certain parts of the sensor field. The actual landing position cannot be controlled due to the existence of wind and obstacles such as trees and buildings. Consequently, the coverage may be inadequate for specific application requirements regardless of how many sensors are dropped.

In these scenarios, it is possible to make use of mobile sensors, which can be made to move to appropriate locations to provide the required coverage. Mobility can significantly increase the capability of a sensor network by making it resilient to failures, react

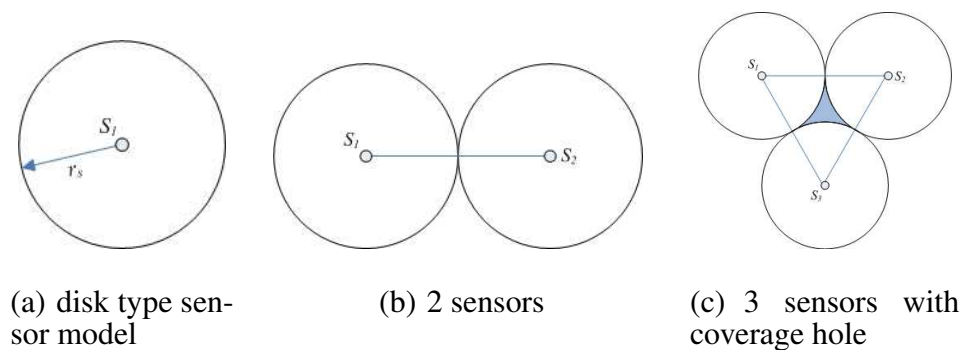


Fig. 1. Sensor model and coverage

to events, and be able to support disparate missions with a common set of sensors. Multiple mobile agents provide us with a flexible, robust and distributed solution for data collection in sensor networks.

Sensor deployment is basically an optimal sensor location problem. Let us consider a binary sensor model which is a disk model as shown in fig. 1(a), and define r_s as its sensing range. The aim of the sensor network is to maximize the area covered by placing multiple sensors in the environment. When there are more than 2 sensors, an optimization problem arises. For example, we can maximize the coverage area by arranging two disks adjacent to each other as shown in fig. 1(b). With more than 3 sensors, which is generally true in sensor networks, there may exist a coverage hole (void) between sensors as shown in fig. 1(c) (colored area in the middle of the three sensors). To remove this void, we may overlap sensor detection areas. In this case, we need to minimize the overlapped area to maximize the covered area for a given number of sensors.

Let us define d_s as the distance between two sensors. Then,

$$d_s = \sqrt{(x_i - x_j)^2 + (y_i - y_j)^2}, \quad (2.4)$$

where (x_i, y_i) and (x_j, y_j) are two sensor positions in 2-D space. In a two sensor case, it is simply $2r_s$ to maximize coverage area and minimize the communication range. Let us

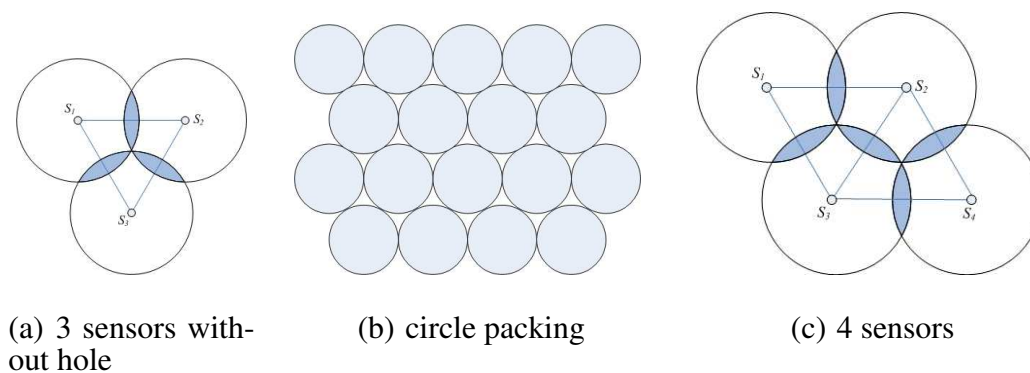


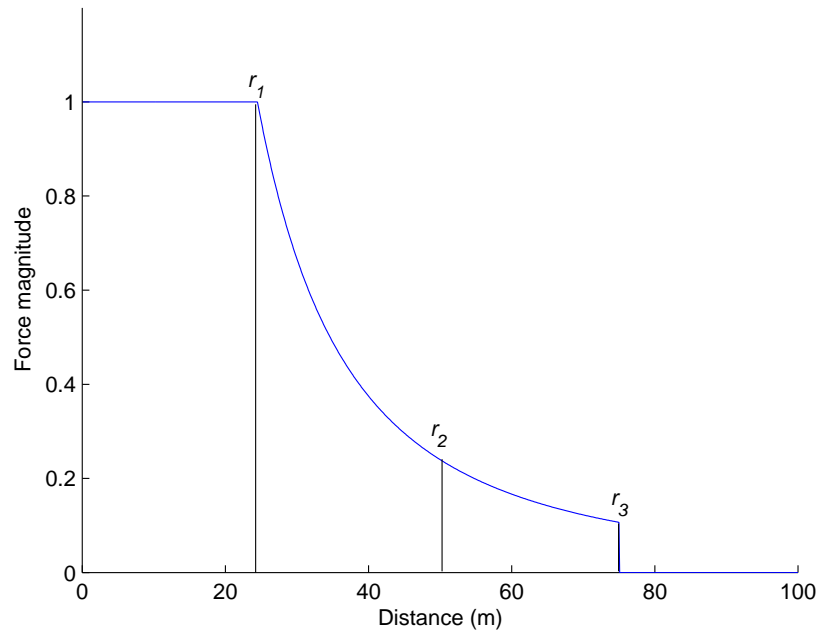
Fig. 2. Optimal placement using disk packing problem

now consider the triangle shown in fig. 2(a). As every d_s is the same, the triangle is an equilateral and from simple geometry, we know d_s is $\sqrt{3}r_s$. The optimal placement of sensors is then the traditional circle packing problem for circles whose radii are $\sqrt{3}r/2$ [15, 16]. A circle packing is an arrangement of circles inside a given boundary such that no two overlap and some (or all) of them are mutually tangent. The densest packing of circles in the plane is the regular hexagonal lattice arrangement, which has a packing density of $\sqrt{3}\pi/6$ as shown in fig. 2(b). The overlapped area (A_o) between two circle in fig. 2(a) is $2(\pi/6 - \sqrt{3}/4)r^2$. In case of four sensors, there are 5 overlapped area as in fig. 2(c). The optimal deployment minimizes such an overlapped area.

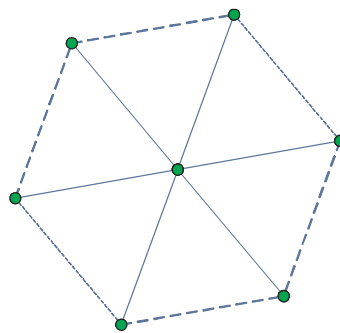
1. Hexagonal deployment

We have so far shown that a hexagonal structure is optimal in terms of our coverage definition. The main problem now is how one should propagate the hexagonal configuration in a distributed manner.

To successfully reach the goal of networked systems, mobile nodes should communicate with each other. In general, a mobile sensor node has a limited range of communication. Therefore, only nodes which are sufficiently close to each other, can establish communication, and the communication topology is strongly influenced by node motion.



(a) force model



(b) hexagonal structure

Fig. 3. Force model and hexagonal structure

Let x_i be the position vector of the i -th node in 2-D and N be the number of nodes, and assume each node has standard second order linear dynamics. We can define $r_{ij} = |x_{ij}|$ as the distance between the i -th node and the j -th node, and we construct a potential function $V(r_{ij})$, which is a function of the distance between two nodes. The control input to a node is the force F_{ij} exerted on the i -th node by the j -th node. It is useful to write the force as the negative gradient of the potential field. Therefore, the total force on each node can be described as

$$F_i = \sum_{j \neq i}^N F_{ij} = - \sum_{j \neq i}^N \nabla V(r_{ij}). \quad (2.5)$$

The magnitude of the force as a function of the distance is shown in fig. 3. It is necessary to adjust the magnitude of the force to the feasible level to accommodate control input saturation. This limit is set as F_{max} , and comes into play when $r \leq r_1$. The force is repulsive if $r \leq r_2$, and attractive if $r \geq r_2$. There is no force exerted if $r \geq r_3$. In this work, the potential field is chosen so that the force function is of the form

$$F_{ij} = \frac{\alpha}{r_{ij}^\beta}, \quad (2.6)$$

where α and β are the parameters we can tune. Each node uses exactly the same control law because the nodes are assumed to be identical, and are influenced only by the neighboring nodes, i.e., those within a ball of radius r_3 . The global minimum of the sum of all the potentials consists of a configuration in which neighboring nodes are spaced equally at a distance r_2 from one another as shown in fig. 3(b).

For a uniform distribution of the sensor nodes, the hexagonality of a deployment can be measured by uniformity. Uniformity is defined as the average of the local standard deviation of the distances between neighboring nodes [17]. Let \mathcal{N}_i be a set of nodes which can communicate with and be detected by the i -th node. Then, the overall uniformity of a

deployment is

$$U = \frac{1}{N} \sum_{i=1}^N U_i$$

$$U_i = \left(\frac{1}{|\mathcal{N}_i|} \sum_{j \in \mathcal{N}_i} (|x_{ij}| - \mu_i)^2 \right)^{\frac{1}{2}}$$

where U_i is the local uniformity, and μ is the mean of the distances between the i -th node and its neighbors. A smaller value of U means that the nodes are more uniformly placed, and with our force model, the deployment has a hexagonal structure.

The main problem of this form of artificial force is that the system has discontinuous right hand side. The sign of the force switches at a certain distance r_2 . A node is locally interacting with neighbors, and each node is governed by discontinuous differential equations. Therefore, stability analysis is required for the overall network.

C. Stability Analysis for Time Invariant System

We define the state of the n nodes as $x=(x_1, \dots, x_n, \dot{x}_1, \dots, \dot{x}_n)$. Let us consider an undirected neighboring graph, $\mathcal{G} = \{\mathcal{V}, \mathcal{E}\}$, which is composed of as a finite non-empty set of vertices, $\mathcal{V} = \{x_1, x_2, \dots, x_n\}$, and a finite set of edges, $\mathcal{E} = \{e_{ij} | (x_i, x_j) \in \mathcal{V} \times \mathcal{V}, x_i \sim x_j\}$ (fig. 4). A vertex represents a mobile node and an edge contains unordered pairs of nodes that depict neighborhood between the nodes. We now define a neighboring set of node i , $\mathcal{N}_i = \{j | (x_i, x_j) \in \mathcal{E}, |x_i - x_j| \leq r_r, r_c\}$, as a set of nodes which can communicate with and be detected by node i . It is proved that if $r_c \geq 2r_r$, complete coverage of a convex region implies connectivity of an arbitrary network [18]. We assume the same condition here so that connectivity is always guaranteed. First, we consider the time invariant case, where a node can communicate with all other nodes or a set of neighboring nodes \mathcal{N}_i does not change. This property induces that the total potential energy of the group is differentiable as long as the potential energy function for each node is differentiable. Then the control

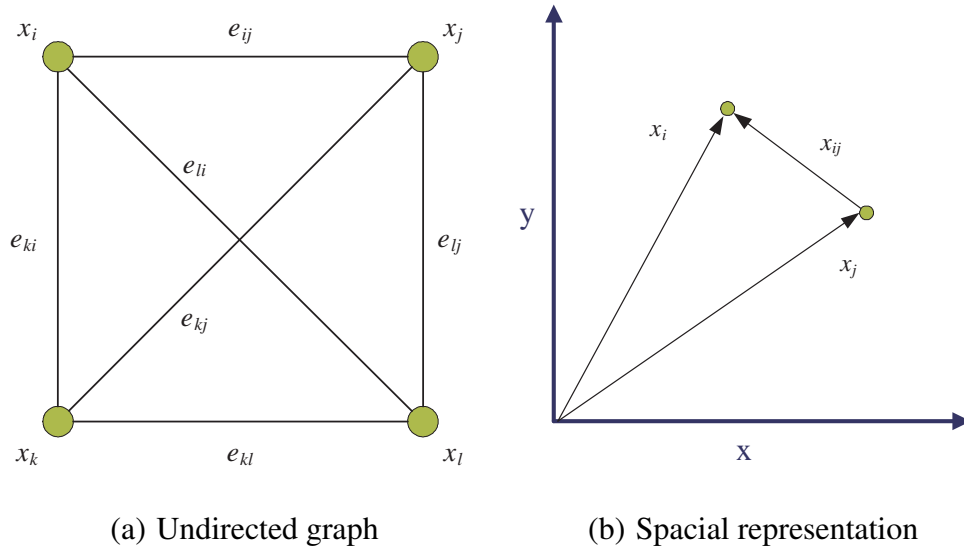


Fig. 4. Undirected graph and its spacial representation

input to a node is smooth and classic Lyapunov stability theory can be applied.

Let us consider a continuously differentiable Lyapunov function (Φ) that combines kinetic energy and potential energy in the form

$$\Phi = \frac{1}{2} \sum_{i=1}^n \left(\dot{x}_i^T \cdot \dot{x}_i + \sum_{j \in \mathcal{N}} V(x_{ij}) \right). \quad (2.7)$$

Let us define a set Ω as

$$\Omega = \{(x, \dot{x}) | \Phi \leq \phi\}, \forall i, j \in \{1, \dots, n\}, \quad (2.8)$$

for a sufficiently large value of ϕ . The set, for $\phi > 0$, is closed by continuity. Because of the symmetric property of $V(x_{ij})$ and $V(x_{ji})$, and the property of $x_{ij} = -x_{ji}$,

$$\frac{\partial V_{ij}}{\partial x_{ij}} = \frac{\partial V_{ij}}{\partial x_i} = -\frac{\partial V_{ij}}{\partial x_j} \quad (2.9)$$

Therefore, the time derivative of the potential energy becomes

$$\frac{d}{dt} \sum_{j \in \mathcal{N}} V(x_{ij}) = \sum_{j \in \mathcal{N}} (\dot{V}_{ij}) = \sum_{j \in \mathcal{N}} \dot{x}_{ij}^T \nabla V(x_{ij}) = 2 \sum_{j \in \mathcal{N}} \dot{x}_i^T \cdot \nabla V(x_{ij}). \quad (2.10)$$

And, the time derivative of Φ becomes

$$\dot{\Phi} = \sum_{i=1}^n \dot{x}_i^T \cdot \left(\ddot{x}_i + \sum_{j \in \mathcal{N}} \nabla V(x_{ij}) \right). \quad (2.11)$$

For simplicity, let us consider a simple unit mass dynamics system for a node.

$$\ddot{x}_i = u_i - c\dot{x}_i. \quad (2.12)$$

Because we are considering control input u as the negative gradient of the potential, equation 2.11 can be expressed as

$$\dot{\Phi} = \sum_{i=1}^n \dot{x}_i^T \cdot \left(-c\dot{x}_i - \sum_{j \in \mathcal{N}} \nabla V(x_{ij}) + \sum_{j \in \mathcal{N}} \nabla V(x_{ij}) \right) \quad (2.13)$$

$$= -c \sum_{i=1}^n \dot{x}_i^T \cdot \dot{x}_i. \quad (2.14)$$

For the positive damping coefficient c , $\dot{\Phi}$ is semi-negative definite ($\dot{\Phi} \leq 0$). Equality $\dot{\Phi} = 0$ holds only when $\dot{x}_i = 0$. Therefore, the system with the given control law is asymptotically stable. Let \mathcal{S} be the invariant set in Ω

$$\mathcal{S} = \{(x, \dot{x}) | \dot{\Phi} = 0\}. \quad (2.15)$$

From LaSalle's invariance principle, we can conclude that the nodes will converge to the largest invariant set in \mathcal{S} . However, with nonzero c , $\dot{\Phi}$ is zero only when all the nodes are at rest. We do not consider the trivial case, in which a node is at rest because there is no node within given sensing range. Therefore, the above statement means that all the distances of neighboring nodes are the same, where the local minima of the potentials are achieved.

CHAPTER III

STABILITY ANALYSIS FOR DISCONTINUOUS DYNAMIC SYSTEM

In this chapter, discussed is the stability of the discontinuous dynamic system. In section A, we first introduce basic preliminaries about nonsmooth vector fields, and Lyapunov stability analysis with nonsmooth Lyapunov functions. The framework used was developed by Shevitz and Paden [14]. In the following section, we prove the stability of the system which has a discontinuous right hand side and has a hexagonal structure as discussed in the previous chapter.

A. Preliminaries

1. Piecewise smooth vector field

In many cases, vector fields may be smooth only over a finite number of regions. A discontinuous jump may occur at the switching boundary. Let us define switching boundary $\mathbb{B} \subset R^n$ as

$$\mathbf{G} = \{x \in R^n \mid \mathbf{g}(x) = 0\} \quad (3.1)$$

where \mathbf{g} is a function $g : R^n \rightarrow R$. $(n - 1)$ dimensional \mathbf{G} splits R^n into two regions

$$\mathbf{G}_+ = \{x \in R^n \mid \mathbf{g}(x) > 0\} \quad (3.2)$$

$$\mathbf{G}_- = \{x \in R^n \mid \mathbf{g}(x) < 0\} \quad (3.3)$$

Figure 5 shows examples of piecewise smooth vector fields. Let us assume that $g(x)$ is smooth in \mathbf{G}_+ and \mathbf{G}_- but is discontinuous at \mathbf{G} . To determine a solution trajectory for the piecewise smooth vector fields, we will use the Filippov solution concept which will be explained in the next subsection. For the inward flow case, the integral curve moves along

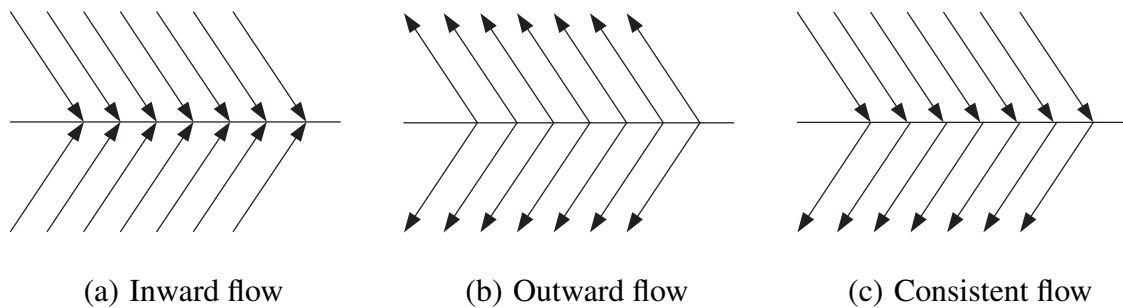


Fig. 5. Piecewise smooth vector field

\mathbf{G} , assuming the vectors inside of \mathbf{G} point in the same direction (within the convex hull) as the vectors on either side of the boundary. In applications, this property may lead physical systems to oscillations around \mathbf{G} . The outward flow case can lead to non-uniqueness if the initial state lies in \mathbf{G} . However, trajectories that start outside of \mathbf{G} will not cross \mathbf{G} , and there will be no such non-uniqueness issues. For the consistent flow case, the vectors at \mathbf{G} must lie between the vectors before and after crossing \mathbf{G} in both magnitudes and directions.

2. Lyapunov stability of nonsmooth systems

We consider the vector differential equation with discontinuous right-hand side given by

$$\dot{x} = f(x), \quad (3.4)$$

where $f : \mathbb{R}^n \rightarrow \mathbb{R}^n$ is measurable and essentially locally bounded. From [19]

Definition A.1 *In the case when n is finite, the vector function $x(\cdot)$ is called a solution of 3.4 in $[t_0, t_1]$ if it is absolutely continuous on $[t_0, t_1]$ and for almost all $t \in [t_0, t_1]$*

$$\dot{x} \in K[f](x)$$

where

$$K[f](x) \equiv \bigcap_{\delta > 0} \bigcap_{\mu N = 0} \overline{\text{co}}f(B(x, \delta) - N) \quad (3.5)$$

$\bigcap_{\mu N=0}$ denotes the intersection over all sets N of Lebesgue measure zero. An equivalent definition is: there exists $N_f \subset R_m$, $\mu N_f = 0$ such that for all $N \subset R_m$, $\mu N = 0$

$$K[f](x) \equiv \overline{co}\{\lim f(x_i) | x_i \rightarrow x, x_i \notin N_f \cup N\}$$

Lyapunov stability theorems have been extended for nonsmooth systems in [14]. The authors use the concept of generalized gradient which for the case of finite-dimensional spaces is given by the following definition.

Definition A.2 Let $V : R^n \rightarrow R^n$ be a locally Lipschitz function. The the generalized gradient of V at x is given by

$$\partial V(x) = \overline{co}\{\lim \nabla V(x) | x \rightarrow x, x \notin \Sigma_V\}$$

where Σ_V is the set of measure zero in R^n where the gradient of V is not defined.

Lyapunov stability theorems for nonsmooth systems require the energy function to be regular. Regularity is based on the concept of generalized derivative which was defined by Clarke [20] as follows

Definition A.3 Let f be Lipschitz near x and v be a vector in R^n . Then, the generalized directional derivative of f at x in the direction of v is defined

$$f^\circ(x; v) = \lim_{y \rightarrow x, t \downarrow 0} \sum \frac{f(y + tv) - f(y)}{t}$$

Lemma A.4 Let f be Lipschitz near x , then

$$f^\circ(x; v) = \max\{\langle \xi, v \rangle | \xi \in \partial f(x)\}$$

Definition A.5 *The function $f(x) : R^m \rightarrow R$ is called regular if*

- 1) *for all v , the usual one-sided directional derivative $f'(x;v)$*
- 2) *for all v , $f'(x;v) = f^\circ(x;v)$*

From [14], the following chain rule provides a calculus for the time derivative of the energy function in the nonsmooth case.

Theorem A.6 *Let $x(\cdot)$ be a Fillipov solution to $\dot{x} = f(x)$ on an interval containing t and $V : R^n \rightarrow R$ be a Lipschitz and regular function. Then $V(x)$ is absolutely continuous, $d/dt(V(x(t)))$ exists almost everywhere (a.e.) and*

$$\frac{d}{dt}V(x(t)) \in^{a.e.} \dot{V}$$

where

$$\dot{V} := \bigcap_{\xi \in \partial V(x(t))} \xi^T \begin{pmatrix} K[f](x(t)) \\ 1 \end{pmatrix}$$

From [14]

Theorem A.7 *Let $\dot{x} = f(x)$ be essentially locally bounded and $0 \in K[f](x)$ in a region $Q \supset \{x \in R^n \mid \|x\| < r\}$. Also, let $V : R^n \rightarrow R$ be a regular function satisfying*

$$V(0) = 0$$

and

$$0 < V_1(\|x\|) \leq V(x) \leq V_2(\|x\|)$$

in Q for some $V_1, V_2 \in$ class \mathcal{K} . Then

- 1) $\dot{V} \leq 0$ in Q implies $x = 0$ is a uniformly stable solution
- 2) If in addition, there exists a class \mathcal{K} function $\omega(\cdot)$ in Q with the property

then the solution $x \equiv 0$ is uniformly asymptotically stable.

We shall use the following nonsmooth version of LaSalle's invariance principle to prove the convergence of the prescribed system: From [14]

Theorem A.8 *Let Σ be a compact set such that every Filippov solution to the autonomous system $\dot{x} = f(x), x(0) = x(t_0)$ starting in Σ is unique and remains in Σ for all $t \geq t_0$. Let $V : \Sigma \rightarrow R$ be a time independent regular function such that $\dot{v} \leq 0$ for all $v \in \dot{V}$ (if \dot{V} is the empty set then this is trivially satisfied). Define $S = \{x \in \Sigma | 0 \in \dot{V}\}$. Then every trajectory in Σ converges to the largest invariant set, M , in the closure of S .*

B. Discontinuous Dynamic Systems

Let us again consider each node with unit mass, and define the state variable

$$\mathbf{x} = [x_1, \dot{x}_1, \dots, x_i, \dot{x}_i, \dots, x_n, \dot{x}_n]^T$$

where $\mathbf{x}_i = [x_i, \dot{x}_i]^T$. Then the agent dynamics can be given by

$$\dot{\mathbf{x}}_i = \boldsymbol{\psi}(\mathbf{x}) + \boldsymbol{\tau}(\mathbf{x}) = f(\mathbf{x}),$$

where $\boldsymbol{\psi}(\mathbf{x})$ is a friction force proportional to the velocity, and $\boldsymbol{\tau}(\mathbf{x})$ is a control input derived from the negative gradient of the system. For the simplest expression,

$$\ddot{x}_i = -c\dot{x}_i - \nabla V,$$

where V is the total potential at x_i due to all the neighboring nodes. The equation appears linear and same as the equation used in the constant topology case which was described in Chapter II. However, what we are considering in this chapter is a system with discontinuous right hand side. In group motion analysis, there are two possibilities that the system has discontinuous dynamics. The first case appears where each node has discontinuous

dynamics, while the second case presents the switching topologies where the neighboring set of a node \mathcal{N}_i varies as time passes. We consider the first case here, while methodology and results of nonsmooth analysis are same for the second one. Then the agent dynamics can be explained with a differential inclusion

$$\dot{\mathbf{x}}_i \in K[f](\mathbf{x})_i$$

At the points of discontinuity, \mathbf{x} lies in the convex closure of the limiting values of the vector field. Therefore,

$$K[f](\mathbf{x}) = [\dot{x}_i, -c\dot{x}_i - \sum_{j \in \mathcal{N}_i} \nabla V_{ij}]$$

Note that we discard sets of measure zero where the gradient of V is not defined. Figure

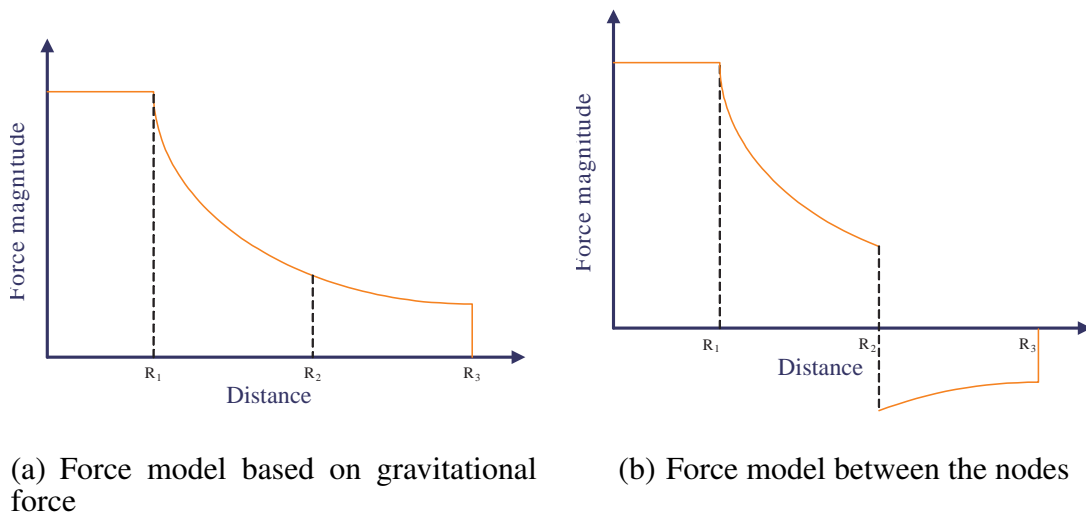


Fig. 6. Force model

6 shows the changes of the force magnitude corresponding to the distance to a neighbor. It is necessary to refine the magnitude of force to feasible level because of control input saturation. This limit is set as F_{max} , and comes into effect when $r \leq R_1$. The force is

repulsive if $r \leq R_2$, and attractive if $r \geq R_2$. There is no force exerted if $r \geq R_3$.

$$F = \begin{cases} F_{max} & \text{if } r < R_1 \\ \frac{G}{r^p} & \text{if } R_1 < r < R_2 \\ -\frac{G}{r^p} & \text{if } R_2 < r < R_3 \\ 0 & \text{if } R_3 < r. \end{cases}$$

Let us consider the nonnegative Lyapunov function candidate

$$\Phi = \frac{1}{2} \sum_{i=1}^n \left(\dot{x}_i^T \cdot \dot{x}_i + \sum_{j \in \mathcal{N}} V(x_{ij}) \right)$$

We now define $V = -\int_r F dr$, which is a negative form for the conventional potential energy along the path so that control input to the system is a negative gradient of the the potential energy. For the force shown in figure 6, we have following potential energy

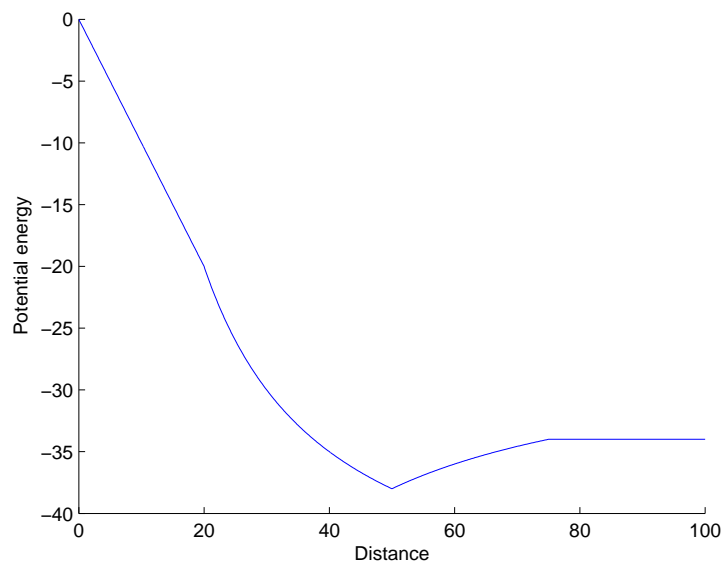
$$V = \begin{cases} -rF_{max} & \text{if } r < R_1 \\ -R_1F_{max} - \frac{G}{(1-p)}r^{(1-p)} + \frac{G}{(1-p)}R_1^{(1-p)} & \text{if } R_1 < r < R_2 \\ -R_1F_{max} - \frac{2G}{(1-p)}R_2^{(1-p)} + \frac{G}{(1-p)}R_1^{(1-p)} + \frac{G}{(1-p)}r^{(1-p)} & \text{if } R_2 < r < R_3 \\ -R_1F_{max} - \frac{2G}{(1-p)}R_2^{(1-p)} + \frac{G}{(1-p)}R_1^{(1-p)} + \frac{G}{(1-p)}R_3^{(1-p)} & \text{if } R_3 < r \end{cases}$$

First two terms in each region are negative for repulsive force whereas the last integral is positive for attractive force. The graphical representation of the potential is shown in figure 7. There are three nonsmooth points in the potential at R_1 , R_2 , and R_3 . The potential values at the discontinuities are

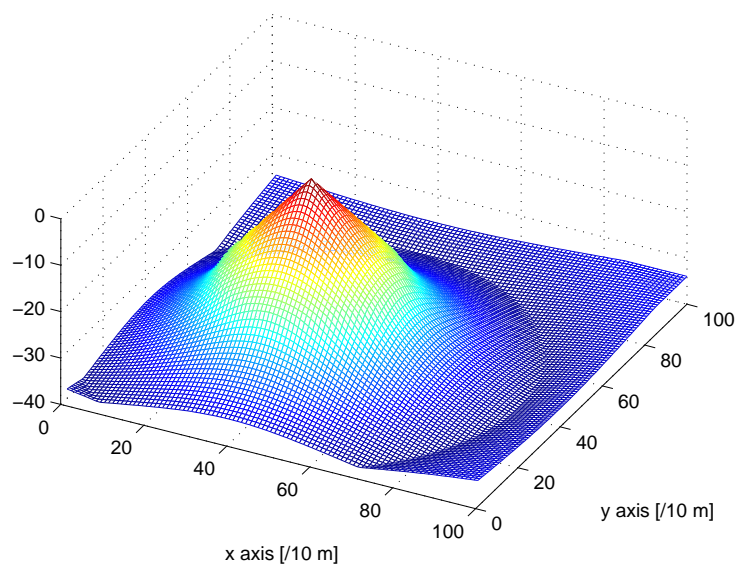
$$V_{R_1} = -R_1F_{max} \quad (3.6)$$

$$V_{R_2} = R_1F_{max} + \frac{G}{(1-p)}R_2^{(1-p)} - \frac{G}{(1-p)}R_1^{(1-p)} \quad (3.7)$$

$$V_{R_3} = -R_1F_{max} - \frac{2G}{(1-p)}R_2^{(1-p)} + \frac{G}{(1-p)}R_1^{(1-p)} + \frac{G}{(1-p)}R_3^{(1-p)} \quad (3.8)$$



(a) Potential energy in 2D plot



(b) Potential energy in 3D plot

Fig. 7. Potential energy derived from the force law

If the distance between two nodes are one of those nonsmooth points ($r \notin \Omega_v$), we need to consider the generalized time derivative of Φ . To apply the nonsmooth version of Lyapunov stability analysis, we need to check the regularity of Φ .

Let us first establish regularities of V at distances which belong to the set of measure zero.

One sided directional derivatives are defined as

$$f'(R_1, v) = \lim_{t \downarrow 0} \frac{V(R_1 + tv)}{V_{R_1}} = \begin{cases} a < 0 & \text{if } v > 0, \\ b > 0 & \text{if } v < 0. \end{cases}$$

$$f'(R_2, v) = \lim_{t \downarrow 0} \frac{V(R_2 + tv)}{V_{R_2}} = \begin{cases} c > 0 & \text{if } v > 0, \\ d < 0 & \text{if } v < 0. \end{cases}$$

$$f'(R_3, v) = \lim_{t \downarrow 0} \frac{V(R_3 + tv)}{V_{R_3}} = \begin{cases} e = 0 & \text{if } v > 0, \\ f < 0 & \text{if } v < 0. \end{cases}$$

Now we define gradient of V where $r \notin \Omega_v$

$$\nabla V(r) = \begin{cases} -\frac{G}{R_1^p} & \text{if } r < R_1 \\ -\frac{G}{r^p} & \text{if } R_1 < r < R_2 \\ \frac{G}{r^p} & \text{if } R_2 < r < R_3 \\ 0 & \text{if } R_3 < r. \end{cases}$$

Note that ∇V includes the derivative with respect to time even though it is not shown in the expression. By combining definition of Glarke's generalized gradient and lemma A.4, we

have

$$f^\circ(R_1, v) = \begin{cases} a < 0 & \text{if } v > 0, \\ b > 0 & \text{if } v < 0. \end{cases}$$

$$f^\circ(R_2, v) = \begin{cases} c > 0 & \text{if } v > 0, \\ d < 0 & \text{if } v < 0. \end{cases}$$

$$f^\circ(R_3, v) = \begin{cases} e = 0 & \text{if } v > 0, \\ f < 0 & \text{if } v < 0. \end{cases}$$

By the definition of regular function, V is regular, and Φ is regular as a sum of regular functions. Regularity and the property of finite sums of generalized gradients provide us

$$\partial\Phi = [\Sigma\partial_{x_1} V_i, \dot{x}_i, \dots, \Sigma\partial_{x_n} V_i, \dot{x}_n]^T$$

From Clarke's chain rule, we have the generalized time derivative of Φ

$$\begin{aligned} \tilde{\Phi} &= \bigcap_{\xi \in \partial\Phi(x(t))} \xi^T (K[f](x(t))) \\ &= \bigcap \Sigma [\dot{x}_i^T \Sigma \partial_{x_i} V - c \dot{x}_i^T \dot{x}_i - \dot{x}_i^T \Sigma \partial_{x_i} V] \\ &= \overline{co} \{-\Sigma c \dot{x}_i^T \dot{x}_i\} \\ &\leq 0. \end{aligned}$$

As we do not consider the trivial case where the graph is not connected, $\tilde{\Phi} = 0$ only when $\dot{x}_i = 0$. Let \mathcal{S} be the invariant set in Ω

$$\mathcal{S} = \{(x, \dot{x}) | \tilde{\Phi} = 0\}. \quad (3.9)$$

From LaSalle's invariance principle, we can conclude that the nodes will converge to the largest invariant set in \mathcal{S} . However, with nonzero c , $\tilde{\Phi}$ is zero only when all the nodes

are at rest. We do not consider the trivial case, in which a node is at rest because there is no node within given sensing range. Therefore, the above statement means that all the distances of neighboring nodes are the same, where the local minima of the potentials are achieved.

CHAPTER IV

HIERARCHICAL NETWORK DEPLOYMENT

In this chapter, presented is the deployment algorithm using a two layered hierarchical structure. Concepts of active and passive nodes are introduced, and the system with those active and passive nodes is analyzed.

A. Clustering in Mobile Sensor Networks

A major approach for collaboration among those with limited capability is to organize the mobile nodes into *groups* which are generally called *clusters*. It enables one to build useful hierarchical structures for mobile nodes. Clustering in mobile sensor networks has been extensively investigated because of the advantages of reduced power, increased distributed nature, and improved adaptability to various environments [21]. Moreover, within a cluster, much simpler protocols can be used to provide the system more efficient ways of using limited resources [22].

In a clustering structure, mobile nodes are classified into one of three classes: head node, gateway node or member node. A cluster head is in charge of coordinating other nodes in its cluster. A cluster gateway is a communication link with neighboring clusters, which forwards information between clusters. A member node is an ordinary node which is not a head nor a cluster link. In the mobile device setting, it is appropriate to assume that the cluster heads are located within the cluster.

1. Clustering scheme

We assume herein that a node is either a head node or a non-head node in a cluster and belongs to only one cluster, which means clusters do not share a node. It is further assumed

that a head node works as a gateway node so that connection links between the clusters are established only between the head nodes. Therefore, the network has a hierarchical structure with two layers: lower layer and upper layer. Nodes at the lower layer are the ordinary member nodes and those in the upper layer are the head nodes.

The clustering schemes have been extensively developed, and they can be classified with different criteria. A broad survey of the schemes is presented in [23]. One criterion used to classify the scheme is the existence of a cluster head, and the hierarchical scheme based on the cluster head can be divided into two categories: (i) where cluster heads are identical to member nodes, or (ii) cluster heads are superior to member nodes. In the first category, all the nodes are assumed to have identical capabilities and energies, and some of them are selected as cluster heads [24]. On the contrary, in the second category, a small number of nodes are equipped with more resources than ordinary members [25].

In our scheme, all the nodes are assumed to be identical. Some of the nodes are randomly selected as cluster heads, and form a hierarchical structure. Then cluster heads form a certain desired formation by upper level potential fields. When they reach the goal positions, the cluster heads become ordinary nodes, and the structure is converted to a flat structure (one layer structure).

While the structure is hierarchical, nodes in a cluster move as a rigid body. In rigid body motion, mobile nodes maintain fixed relative positions while their positions in space change. These fixed relative positions form a *virtual structure* [26],[27]. With this structure, all the nodes in the same cluster moves as a single structure. It is easy to understand that mobile nodes keep the same position with respect to the reference frame which is attached to the cluster head. In defining potentials for the head node or non-head node, we designate the head node as an active node, and the non-head node as a passive node, which will be discussed in the next section.

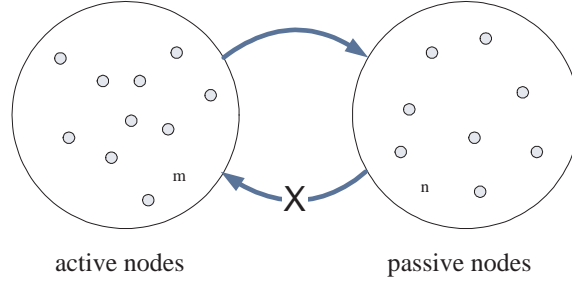


Fig. 8. Concept of active and passive nodes

B. Active Nodes and Passive Nodes

1. Definitions

A Passive node is a mobile sensor unit which is affected by the potential field generated by active nodes, and does not generate any force on an active node (see fig. 8). An active node, on the contrary, is a mobile unit which generates a potential field which has an effect on neighboring nodes. A node in the active nodes group generates forces on nearby nodes in both active and passive nodes groups, while a node in the passive nodes group can only generate a force which affects only the neighboring passive nodes.

Let us consider a mixed neighboring graph, $\mathcal{G} = \{\mathcal{V}, \mathcal{E} \cup \mathcal{A}\}$, which is composed of a finite non-empty set of vertices, $\mathcal{V} = \{x_1, x_2, \dots, x_{m+n}\}$, and a finite set of undirected edges, $\mathcal{E} = \{x_{ij} | (x_i, x_j) \in \mathcal{V} \times \mathcal{V}, x_i \sim x_j\}$, and a finite set of directed arcs \mathcal{A} . Let $\mathcal{C} = \{c_1, \dots, c_m\}$ and $\mathcal{P} = \{p_1, \dots, p_n\}$ be two sets in \mathcal{V} , with $|\mathcal{C}| = m$, $|\mathcal{P}| = n$, $\mathcal{C} \cup \mathcal{P} = \mathcal{V}$ and $\mathcal{C} \cap \mathcal{P} = \{\}$. The undirected edge set $\mathcal{E} = \{(c_i, c_j) \cup (p_k, p_l) | c_{ij} = (c_i, c_j) \in \mathcal{C} \times \mathcal{C}, p_{kl} = (p_k, p_l) \in \mathcal{P} \times \mathcal{P}, c_i \sim c_j, \text{ and } p_k \sim p_l\}$ and the directed arc set $\mathcal{A} = \{a_{ki} = (p_k, c_i) | p_k \in \mathcal{P} \text{ and } c_i \in \mathcal{C}\}$.

We now define two neighboring sets: \mathcal{N}_i^c for the vertices in \mathcal{C} and \mathcal{N}_k^p for the vertices in \mathcal{P} . In this case, a set of neighbors of a vertex in \mathcal{C} is

$$\mathcal{N}_i^c = \{j | (c_i, c_j) \in \mathcal{E}, |c_i \sim c_j| \leq r_r, r_c\}$$

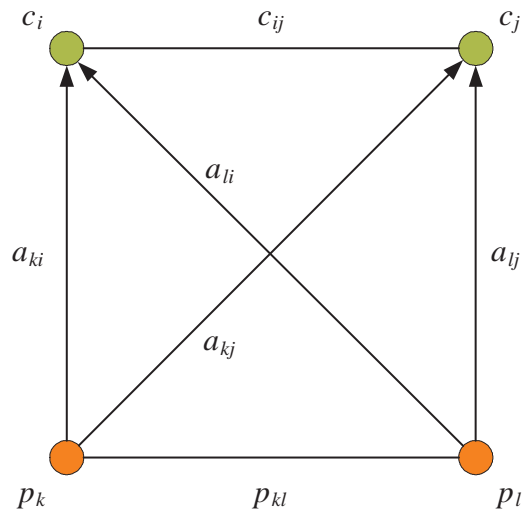


Fig. 9. Mixed (directed and undirected) graph

and a set of neighbors of a vertex in \mathcal{P} is

$$\mathcal{N}_k^p = \{l, i \mid (p_k, p_l) \in \mathcal{E}, (p_k, c_i) \in \mathcal{A}, |p_k \sim p_l| \leq r_r, r_c, \text{ and } |p_k \sim c_i| \leq r_r, r_c\}$$

The notation is illustrated in fig. 9.

For the network analysis, we describe \mathcal{C} as the set of active nodes and \mathcal{P} as the set of passive nodes. From this point on, subscripts a and p denote *active* and *passive*, respectively. For the i th active node, the control input is the sum of negative gradients of the potentials of the neighboring active nodes

$$u_i = - \sum_{j \in \mathcal{N}_i^c} \nabla V_a(c_{ij}) \quad (4.1)$$

where V_a is the potential of the active nodes. For the k th passive node, the control input is the sum of the negative gradients of the neighboring active nodes and the sum of the negative gradients of the neighboring passive nodes

$$u_k = - \sum_{i \in \mathcal{N}_k^p} \nabla V_a(a_{ki}) - \sum_{l \in \mathcal{N}_k^p} \nabla V_p(p_{kl}) \quad (4.2)$$

where V_p is the potential of the passive nodes.

2. Stability analysis

Let us define the state of the $m + n$ nodes as

$$x = (x_1, \dots, x_m, x_{m+1}, \dots, x_{m+n}, \dot{x}_1, \dots, \dot{x}_m, \dot{x}_{m+1}, \dots, \dot{x}_{m+n}).$$

For convenience, we define x_i as

$$x_i = \begin{cases} \text{active node} & \text{if } i \in \{1, 2, \dots, m\} \\ \text{passive node} & \text{if } i \in \{m+1, m+2, \dots, m+n\} \end{cases}$$

Once again, we consider the time invariant case, where a node can communicate with all other nodes or where the set of neighboring nodes \mathcal{N}_i does not change. At the equilibrium states $x = x_{eq}$, we can investigate the stability of the system with an appropriate Lyapunov function.

Let us consider a continuously differentiable Lyapunov function (Φ) with kinetic energy and potential energy which are from the given relative positioning. First, Φ is constructed by summing functions for both active and passive groups.

$$\Phi = \frac{1}{2} \sum_{i=1}^m (\dot{x}_i^T \cdot \dot{x}_i + \sum_{j \in \mathcal{N}_i^c} V_a(x_{ij})) + \frac{1}{2} \sum_{i=m+1}^{m+n} (\dot{x}_i^T \cdot \dot{x}_i + \sum_{j \in \mathcal{N}_i^p} V_a(x_{ij}) + \sum_{k \in \mathcal{N}_i^p} V_p(x_{ki})) \quad (4.3)$$

Then, time derivative of the Lyapunov function becomes,

$$\dot{\Phi} = \sum_{\alpha=1}^m \dot{x}_\alpha^T \cdot \left(\ddot{x}_i + \sum_{j \in \mathcal{N}_i^c} \nabla V(x_{ij}) \right) + \sum_{i=m+1}^{m+n} \dot{x}_i^T \cdot \left(\ddot{x}_i + \sum_{j \in \mathcal{N}_i^p} \nabla V_a(x_{ij}) + \sum_{k \in \mathcal{N}_i^p} \nabla V_p(x_{ki}) \right) \quad (4.4)$$

Let us again consider simple unit mass dynamics system for a node x_i as in eqn. 2.12.

$$\ddot{x}_i = u_i - c\dot{x}_i \quad (4.5)$$

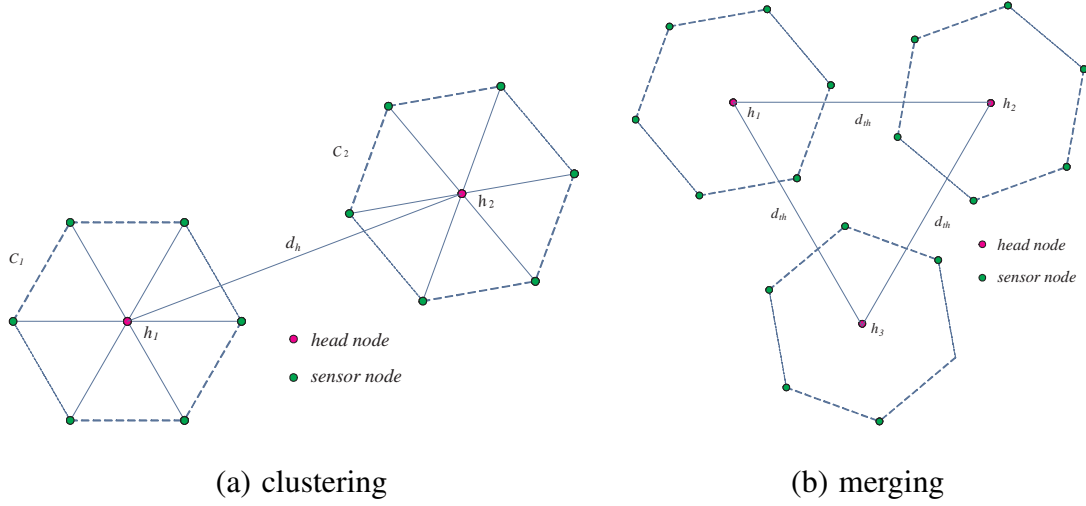


Fig. 10. Clusters and merging

Note that the above equation is applied to both active nodes and passive nodes as u_i differs based on i as described in eqn. 4.1 and 4.2. With the symmetry properties of potential in same groups, the equation can now be described as

$$\begin{aligned}
 \dot{\Phi} &= \sum_{i=1}^m \dot{x}_i^T \cdot \left(u_i - c_i \dot{x}_i + \sum_{j \in N_i^c} \nabla V(x_{ij}) \right) \\
 &\quad + \sum_{i=m+1}^{m+n} \dot{x}_i^T \cdot \left(u_i - c_i \dot{x}_i + \sum_{j \in N_i^p} \nabla V_a(x_{ij}) + \sum_{k \in N_i^p} \nabla V_p(x_{ki}) \right) \\
 &= - \sum_{i=1}^m c_i \dot{x}_i^T \cdot \dot{x}_i - \sum_{i=m+1}^{m+n} c_i \dot{x}_i^T \cdot \dot{x}_i \\
 &= - \sum_{i=1}^{m+n} c_i \dot{x}_i^T \cdot \dot{x}_i
 \end{aligned} \tag{4.6}$$

Therefore, with the positive damping coefficient c_i for every node, $\dot{\Phi}$ is negative semidefinite. Equality $\dot{\Phi} = 0$ holds only when $\dot{x}_i = 0$. Therefore, the system with the given control is asymptotically stable.

3. Forming clusters and merging

Figure 10(a) shows the concept of forming clusters (C_1 and C_2). Each cluster has its cluster head (h_1 and h_2) which is separated from each other by a distance d_h . The deployment scheme consists of three hierarchical steps. First, each cluster determines its head and makes a hexagonal structure as described in the previous section. Then cluster heads establish communication between neighbors within range, and second potential field approach is used to maintain the predefined distance (d_{th} : threshold distance) between them. In this stage, each cluster moves as a rigid body, and ignores the first potential field to nodes in other clusters. Lastly, we cease the second potential, and reapply the first potential to all sensor nodes to construct the final hexagonal structure. We consider the form of the second potential field $V_2(d_h)$ that yields an attractive force which is switched on when $d_h \leq d_{th}$. If d_{th} is set too small, it is possible for the clusters to get tangled, which may cause a collision because the clusters are moving as rigid bodies. If too large, the adjacent nodes between clusters will be out of the communication range. Then, the overall hexagonal structure cannot be accomplished in the third step. Therefore, d_{th} is set to $2.5r_2$ to satisfy the above conditions.

Initial deployment of sensor nodes in a multiple number of groups is feasible as is the case when an airplane drops multiple groups in different places. The only condition is that each group should be located within their maximum communication range.

C. Simulation Results

In this section, we present simulation results for the hexagonal formation via the artificial force from potential, and for the hierarchical formation control. The main purpose of this kind of coverage is to get maximum coverage without coverage hole.

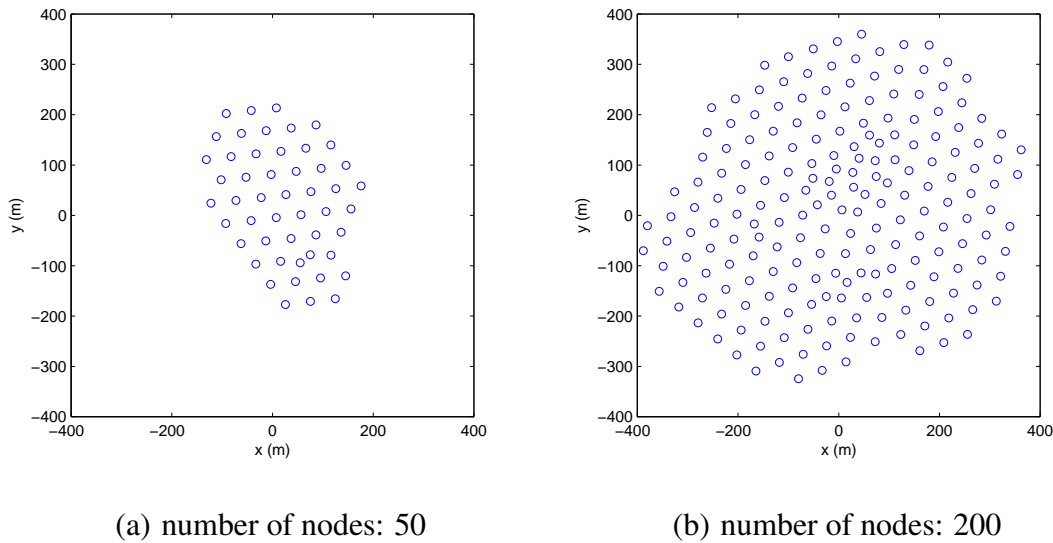


Fig. 11. Hexagonal structure construction

1. Hexagonal structure formation

Figure 11 shows the results from a hexagonal formation of 50 mobile sensor nodes (fig. 11(a)) and 200 nodes (fig. 11(b)). In this simulation, α and β are 500 and 2, respectively, desired equilibrium distance r_2 is 50m, and F_{max} is limited to be 1. The sampling time (δt) is 0.1 sec. and the number of iterations is 6000 so that the total time for the deployment is 10 minutes. Figure 11(a) shows an example of a hexagonal formation. Note however, that the hexagonal structure is not perfect. There are a small number of nodes lumped in the lower right corner. The perimeter of the structure is not hexagonal. These defects are inevitable in our potential based force model, because we are not considering a global controller which can shape the whole system. The overall formation shows, however, well-defined hexagons. It is noticeable that we have quite different results as α and β in equation 2.6 are varied. The effect of different α values is shown in fig. 12. α is too low in fig. 12(a) and too high in fig. 12(b). If α is too low, the overall performance is poor and the system does not converge to a hexagonal structure. If too high, multiple nodes merge into one position, and

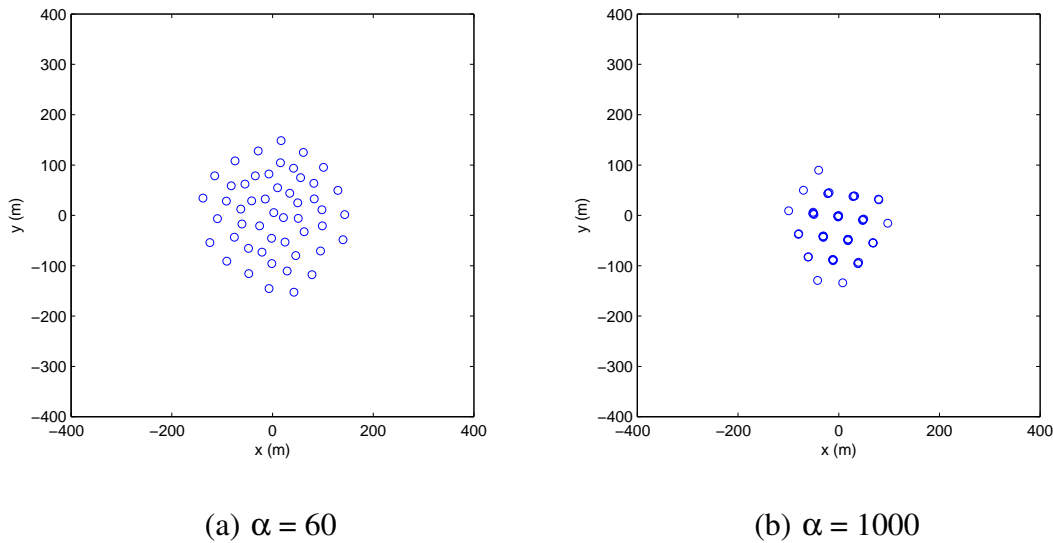


Fig. 12. Effect of different values of α

the nodes are inseparable. The shape of the force model, more fundamentally, the shape of the potential function determines this incompleteness or inseparability. This is because local minima prevent the nodes making hexagonal formation.

The number of nodes also have an effect on the system performance. In terms of overall performance (time and hexagonality), the deployment of 200 nodes shows poorer results compared to the deployment of 50 nodes. The former case takes more time to reach balanced force status in which each node does not move any more. This case also shows a worse hexagonal formation. Even though it is not shown in this dissertation, it can be proved by showing average bearing angles for 3 nodes. In an ideal formation, the angle should be $\pi/3$.

2. Hierarchical application for deployment

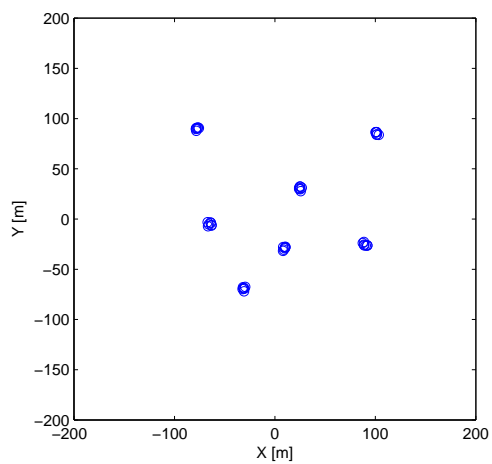
The application of hierarchical structure for node deployment is shown in fig. 13. Seven groups are randomly and uniformly scattered in the $300m \times 300m$ environment (fig. 13(a)). Within each group, 7 mobile nodes are uniformly and randomly distributed in a $5m \times 5m$

square. Each group forms a cluster and a node becomes a cluster head. Cluster heads are active nodes influenced by the potential given in eqn. 4.1, and non-head nodes are passive nodes governed by the potentials given in eqn. 4.2. With these potentials, a cluster makes a hexagonal structure (fig. 13(b)).

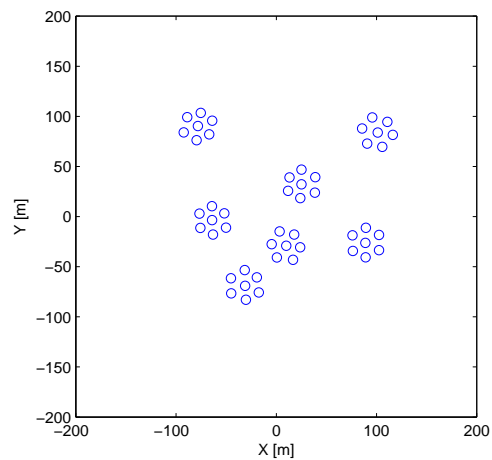
A cluster head establishes a communication link with neighboring cluster heads, and the clusters move as rigid bodies (virtual structures). Potential field based deployment strategy enters the second stage, where only cluster heads are under the influence of the potential (fig. 13(c)). Threshold distance (d_{th}) is set as $2.5r_2$. When cluster heads form the hexagonal structure, the third stage strategy is employed, and every node is influenced by the potentials used in the first stage deployment. In this third stage, all the nodes are passive nodes, which finally form the hexagonal structure as in (fig. 13(d)). Same values are used for the parameters.

The general shape of the deployment in fig. 13(d) is better than the one in fig. 11(a). This is because the nodes in fig. 13(d) are more uniformly distributed in the initial position in fig. 13(b). This more uniform initial positions reduce the probability of the system falling into a deadlock because of the local minima of the given potential.

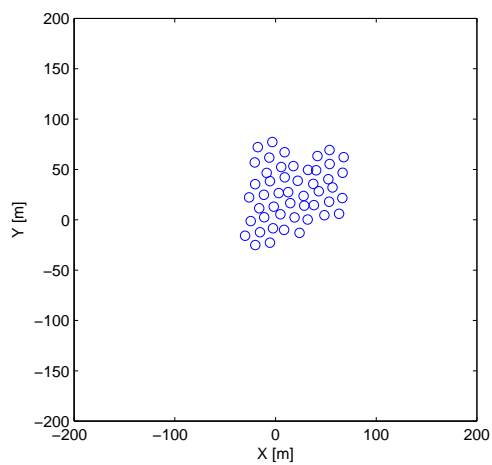
Performance enhancement over the conventional incremental algorithm [28] is shown in fig. 14. For the incremental algorithm, the sensor nodes are initially deployed in $10m \times 10m$ environment. For different number of nodes, simulations are repeated 20 times and the mean values are plotted (fig. 14). For a particular number of nodes, same run times (and hence same number of time steps) are used for both cases. In the incremental case, uniformity deteriorates as the number of nodes are increased, while the hierarchal algorithm provides almost constant uniformity.



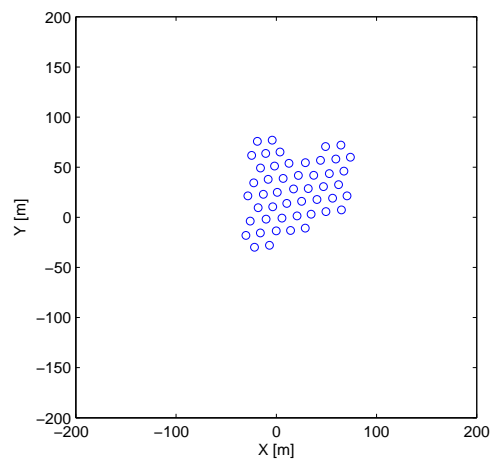
(a) initial deployment



(b) cluster formation



(c) second force field



(d) merging

Fig. 13. Deployment sequence

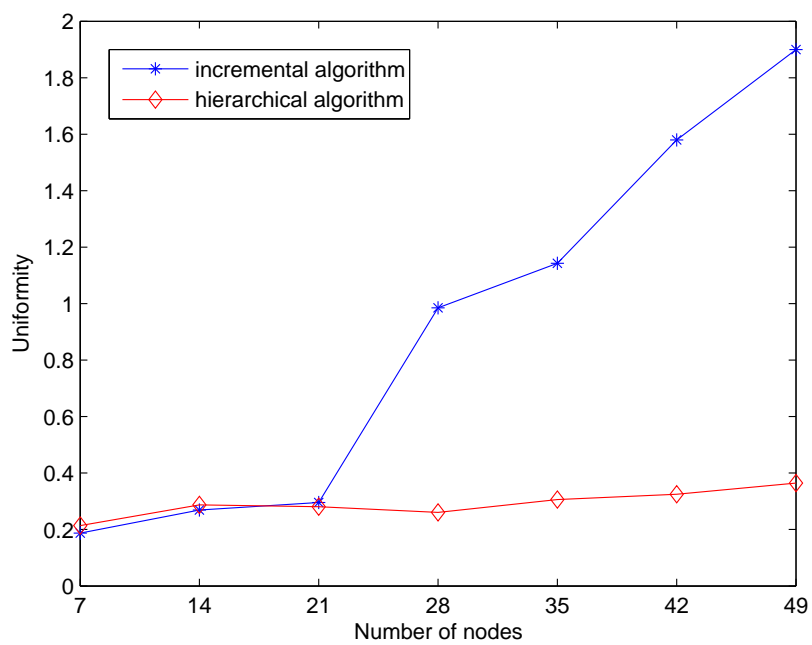


Fig. 14. Performance comparison between the incremental and hierarchical algorithms in terms of uniformity

CHAPTER V

COVERAGE MAINTENANCE FOR TIME VARYING SYSTEM

Once we have completed the initial deployment, the next mission is to maintain the coverage without any failure. To this end, introduced in this chapter is a stochastic sensor model which reflects the decay in sensor performance as the distance from the sensor increases. Also considered is a time varying sensor model with a power alert system to have adaptive network maintenance.

A. Coverage Maintenance

1. Stochastic sensor model

A binary disk type sensor model [29] assumes that the probability of detection within the sensor range r_i is one, and zero outside. However, in reality, sensor detection accuracy deteriorates as the distance from the sensor increases. Therefore, it is necessary to employ a more realistic sensor model to represent this degradation. The most widely used sensor model is an exponentially decaying function according to the distance from the sensor. We modify the stochastic sensor model proposed in [13, 30] and [31]. We start by denoting the sensor detection range of i th sensor (s_i) as r_i . For a sensor s_i at (x_i, y_i) , we can find a point p inside a circular sensing area A_i which is centered at s_i with radius r_i . If we denote $d(s_i, p)$ as the Euclidean distance between s_i and p , then the probability of detection P_d of s_i at p for a binary sensor model can be expressed as

$$P_d(p, s_i) = \begin{cases} 1 & \text{if } d(s_i, p) < r_i \\ 0 & \text{otherwise} \end{cases} \quad (5.1)$$

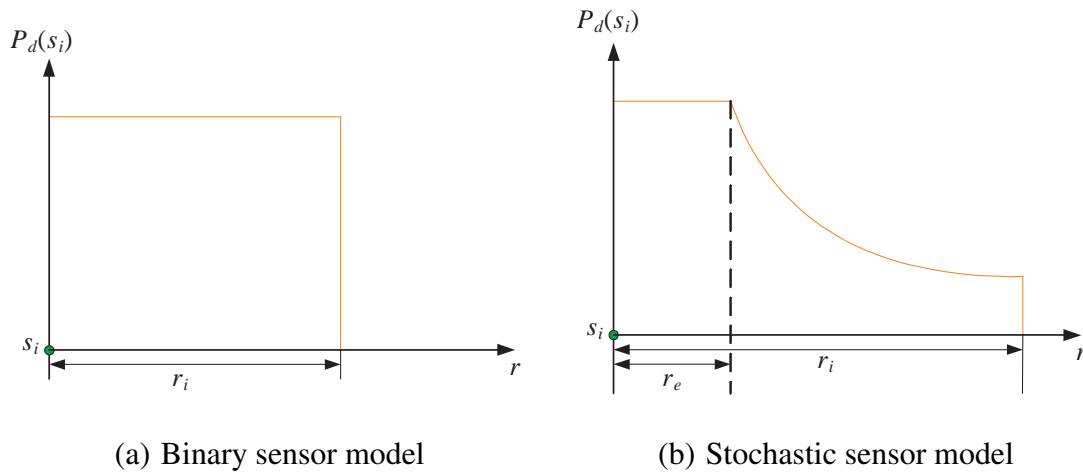


Fig. 15. Sensor models

For a stochastic sensor model, we can express P_d as

$$P_d(p, s_j) = \begin{cases} 0 & \text{if } d(s_i, p) \geq r_i \\ e^{-\lambda\mu^v} & \text{if } r_e < d(s_i, p) < r_i \\ 1 & \text{if } d(s_i, p) \leq r_e \end{cases}, \quad (5.2)$$

where $\mu = d(s_i, p) - r_e$. r_e is the confidence level within which the detection probability keeps its maximum value. For the stochastic sensor model, we define the sensing range of a sensor as $r_i = r_e + \mu$. r_i is the maximum physical sensor range. Variable μ is introduced so that the decaying function for every node is the same when λ and v are fixed. λ and v are parameters that determine the detection probability when a target is at a distance greater than r_e but within the detection range r_i from the sensor. Henceforth, we simply denote $P_d(p, s_i)$ by $P_d(s_i)$. The maximum detection probability is set to 1 when $d(s_i, p) < r_e$ and minimum 0 when $d(s_i, p) > r_i$. In some types of sensors, detection probability means the reliability of information from sensors. Detection necessarily means the identification a movement of an intruder in the network or monitoring an event. We consider a generalized sensor model without particular attention to the reliability of the sensor data. Figure 15 shows these binary and stochastic sensor models characterized by equations 5.1 and 5.2.

Now, we define $P_d(s_i, s_j)$ as the detection probability of being observed by two adjacent sensors s_i and s_j at a valid position p either within A_i or A_j . As shown in figure 16, cumulative probability at a position p is assumed to be some summation of probabilities at that point. Because the detection is independent of one another, for a 2 node case, we can write

$$P_d(s_i, s_j) = 1 - (1 - P_d(s_i))(1 - P_d(s_j)), \quad (5.3)$$

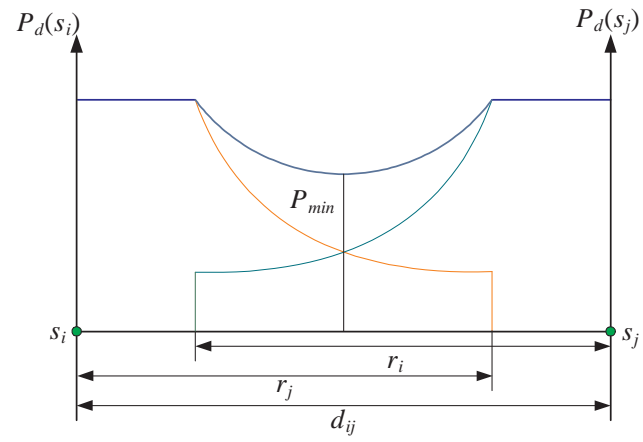
where $(1 - P_d(s_i))(1 - P_d(s_j))$ is the probability that neither s_i nor s_j covers the position p . For ' n ' nodes, we can generalize the detection probability to

$$P_d(s_i, s_j, \dots, s_n) = 1 - \prod_{i=0}^n (1 - P_d(s_i)) \quad (5.4)$$

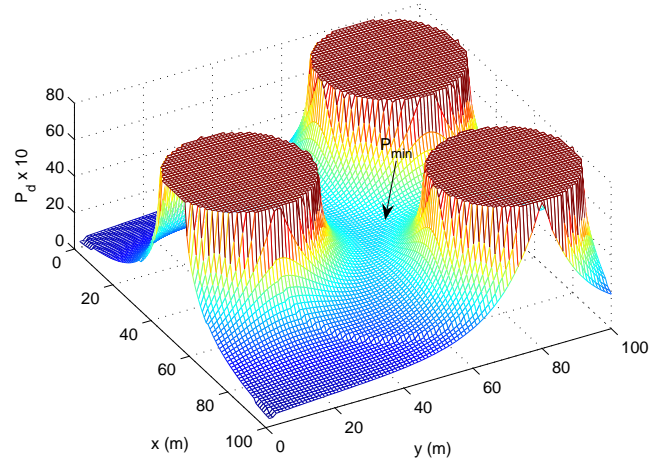
Next, we define P_{th} as a threshold we want to enforce for proper detection. It means

$$\min P_d(s_i, s_j) \geq P_{th}. \quad (5.5)$$

To preserve this property, we need to redefine d_{ij} between s_i and s_j . d_{ij} is determined so that the detection probability at any point between s_i and s_j is larger than P_{th} . Let us begin with the 2 nodes case. The specific value of d_{ij} varies with the parameters defined in equation 5.2. This redefined d_{ij} is now the new distance which should be kept between two sensor nodes s_i and s_j force equilibrium. For simplicity, let us begin with the case that each node has the same power level E . We assume that λ and v stay constant all the time. To determine d_{ij} , we have to get μ . The minimum detection probability appears at the point where P_d values are the same for both sensors s_i and s_j . It means that $P_d(s_i)$ and $P_d(s_j)$ are equal at a point where $P_d(s_i, s_j)$ has its minimum value. This is because $(1 - P_d(s_i))(1 - P_d(s_j))$ is a maximum when $P_d(s_i)$ equals to $P_d(s_j)$. (Note that we are considering a 1-D case, shown in fig. 16(a).)



(a) 2 nodes



(b) 3 nodes

Fig. 16. Cumulative probability distributions

At the position p , where cumulative probability has minimum value, we have

$$1 - (1 - P_d)(1 - P_d) = P_{th}, \quad (5.6)$$

where $P_d = P_d(s_i) = P_d(s_j)$. After some algebra, we have two possible values for P_d of $1 \pm \sqrt{1 - P_{th}}$. As P_d is smaller than 1, P_d is now $1 - \sqrt{1 - P_{th}}$. Let us denote this value as the modified index of probability $P_m (=1 - \sqrt{1 - P_{th}})$. To calculate the sensing range of a sensor (r_i) corresponding to P_m , we have

$$e^{-\lambda\mu^v} = P_m \quad (5.7)$$

After some calculations, we have

$$\mu^v = -\frac{1}{\lambda} \ln P_m \quad (5.8)$$

$$\mu = \left(-\frac{1}{\lambda} \ln P_m\right)^{\frac{1}{v}} \quad (5.9)$$

Now, $d(s_i, p) = d(s_j, p) = r_i = r_e + \mu$. Therefore, the desired distance between those two nodes (d_{ij}) becomes,

$$d_{ij} = d(s_i, p) + d(s_j, p) \quad (5.10)$$

$$= 2r_e + 2\mu \quad (5.11)$$

$$= 2r_e + 2\left(-\frac{1}{\lambda} \ln P_m\right)^{\frac{1}{v}} \quad (5.12)$$

By maintaining this desired distance, any point on the line of sight between s_i and s_j has more detection probability compared to the threshold value. It is important to note that the purpose of this algorithm is not to maintain the threshold detection probability over the entire coverage area. The distance derived from the above equations is for the line of sight between two nodes. In figure 16(b), a minimum detection probability does not exist on the triangular lines made by connecting 3 sensors. The position of minimum detection

probability is not fixed and it depends on the locations of legitimate sensor nodes. Note that we are considering a distributed sensor network system without global information. Two neighboring sensors s_i and s_j are supposed to exchange their sensing range and generate d_{ij} between them. This d_{ij} is the distance to be kept by the artificial force. To be fully autonomous, there cannot be a central unit to adjust sensing ranges between more than 3 sensors. And that is the main difficulty in getting the best distances for more than 3 sensors. Overall performance of the network will be discussed in a later section.

2. Unequal sensor ranges

A homogeneous sensor model has been considered, where all the sensors have identical detection probability within a specified sensing range. Due to hardware differences, however, sensor performance may not be same for every sensor. A different detection model is considered for each sensor node, and the detection range is typically adjusted for each sensor. In a binary sensor model, this individual performance modification can be done by adjusting sensing range. For a stochastic sensor model, the model described in eqn. 5.2 is modified, because sensing range is related to the detection probability. A model modification is made by changing r_e for each sensor. In eqn. 5.2, it is assumed that r_e is constant, which no longer is valid to represent different sensor performances for each sensor node. Sensing range r_i is described by r_e and μ . For the modified probability P_m , μ is always the same, and it reduces the complexity of the performance representation. By changing r_e for each node, the overall detection probability shape can be modified. Now, d_{ij} is no longer a constant between two sensors. Such a scenario is shown in fig. 17. For the 3 sensor positions s_i , s_j , and s_k , we now have different sensor detecting ranges r_i , r_j , and r_k . As discussed in the previous subsection, we assume that the probability distribution has the same value of λ and ν for each sensor node, and μ . Let us define $r_e(s_i)$ as the confidence

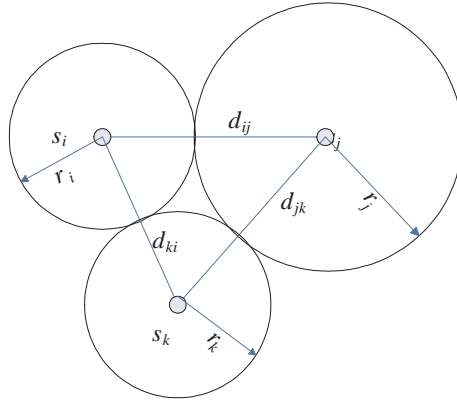


Fig. 17. Nonhomogeneous sensor ranges

level of sensor s_i . Then the sensor model becomes

$$P_d(s_i) = \begin{cases} 0 & \text{if } d(s_i, p) \geq r_i \\ e^{-\lambda \mu^v} & \text{if } r_e(s_i) < d(s_i, p) < r_i \\ 1 & \text{if } d(s_i, p) \leq r_e(s_i) \end{cases}, \quad (5.13)$$

The main difference in this nonhomogeneous case is that each sensor now has a different value of r_e . As $P_d(s_i) = P_d(s_j)$ at p , where $P_d(s_i, s_j)$ is minimum, we have

$$e^{-\lambda \mu_1^v} = e^{-\lambda \mu_2^v} = \frac{1}{2} P_m \quad (5.14)$$

Therefore,

$$\mu_1 = \mu_2 = \left(-\frac{1}{\lambda} \ln P_m\right)^{\frac{1}{v}} \quad (5.15)$$

Now, the distance (d_{ij}) between those two nodes becomes,

$$d_{ij} = d(s_i, p) + d(s_j, p) \quad (5.16)$$

$$= r_e(s_i) + r_e(s_j) + \mu_1 + \mu_2 \quad (5.17)$$

$$= r_e(s_i) + r_e(s_j) + 2\left(-\frac{1}{\lambda} \ln P_m\right)^{\frac{1}{v}} \quad (5.18)$$

$$(5.19)$$

It should be noted that a node now has different distances to its neighboring nodes. Figure

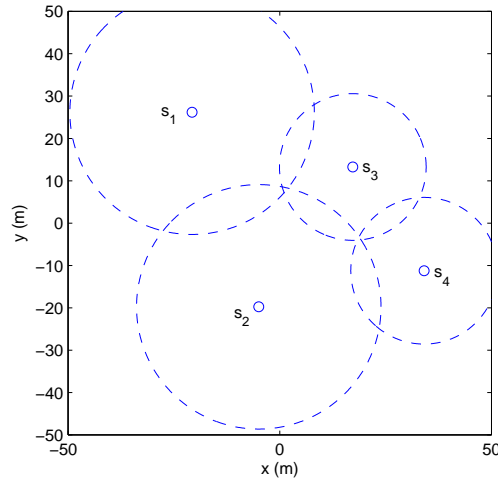


Fig. 18. 4 sensor nodes with 2 different ranges

18 shows an example of 4 nodes, where r_1, r_2 are $25m$, and r_3, r_4 are $15m$.

3. Time varying system

Let us define $E_i(t)$ as the current energy level of a sensor node at time t . Then, r_e is expressed as a function of $E_i(t)$, i.e., $r_e(E_i(t))$. This is to incorporate various power models into the sensor model. Each r_i and r_j is calculated by determining $P(r_i) = P(r_j) = P_d$. And d_{ij} is

$$d_{ij} = r_e(E_i) + r_e(E_j) + 2\left(-\frac{1}{\lambda} \ln P_{th}\right)^{\frac{1}{\nu}} \quad (5.20)$$

The variation of the sensor model due to the change of r_e is shown in fig. 19, where the energy level is directly reflected in r_e . A smaller r_e means a more dissipated energy level of a mobile node. As r_e gets smaller, overall sensor detection probability shifts to the left. Therefore, to keep the detection probability P_m constant with neighboring nodes, the distance d_{ij} needs to be decreased in line with the energy level.

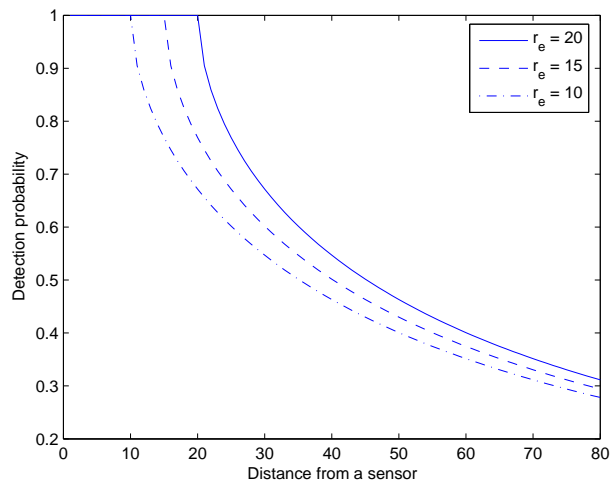


Fig. 19. Changes in sensor performance due to r_e

B. Simulation Results

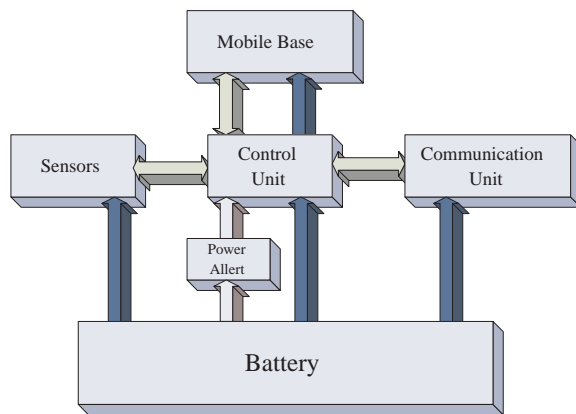


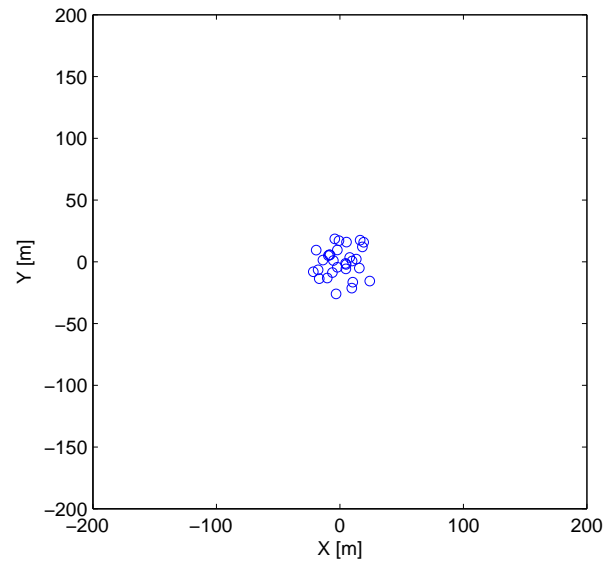
Fig. 20. Mobile sensor unit with power alert

Figure 20 shows a schematic of a mobile sensor unit composed of energy supply and energy consuming units. Central computing unit, sensors, mobile base and communication units are all energy consuming units which are powered by the energy supply unit (battery). The status of the battery is monitored by a power alert unit. The control unit receives signals from the power alert unit and determines the proper energy level $E(t)$, and selects

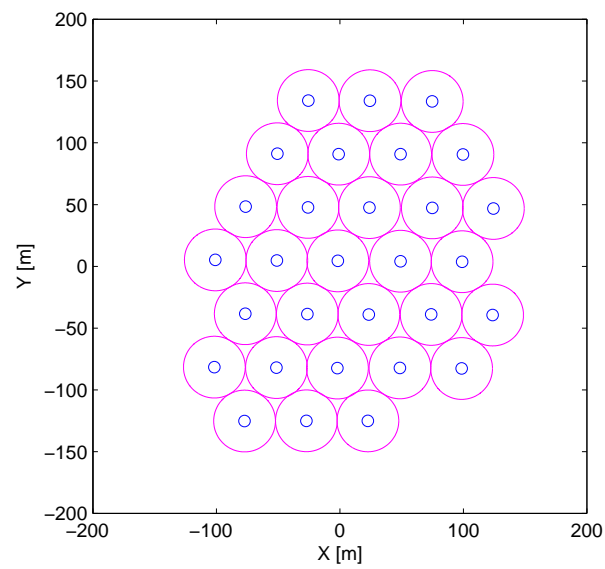
$r_e(t)$. Figure 21 shows the deployment of the homogeneous sensor nodes. Initially, 30 mobile nodes are randomly and uniformly distributed in a 10m by 10m environment (figure 21(a)). Each sensor has the same sensing range (radius of the circle surrounding a node in the figures). The range is the distance with which detection probability can be maintained at a given threshold value (P_m), which is set at 0.7 in this simulation. In the initial deployment, the sensors are assumed to be identical and r is set to 25m. Sensors are deployed with an artificial force model and the deployment is completed in 200 time steps (1 time step = 10 seconds, figure 21(b)).

Figure 22 shows the sensing range, which decays randomly with the power model which decays randomly as well. As time passes, power levels begin to diminish and sensing range for each node gets smaller with regard to its power model. Those performance deteriorations are shown in fig. 23 and fig. 24. For both figures, the same sensing range degradation shown in fig. 22 is applied to the individual sensors. Simulation results here are for the same initial positions and sensing ranges as those in fig. 21(b). Stages 1 and 2 are at the 100th and 150th time steps. We can see that the distance d_{ij} between s_i and s_j is time invariant in fig. 23, while d_{ij} becomes smaller with time in fig. 24.

Figure 25 compares the performance of two algorithms (time invariant and time variant models). The fraction in the figure indicates how much area in the field of interest is observed with a higher detection probability compared to the given threshold P_m . To be consistent in evaluating performances, a new sensing area is defined at each time step. Minimum bounding circle, which contains all the sensor nodes with minimum radius, is chosen as the reference region and fig. 25 shows the fraction of the covered area with respect to the reference region. As time passes, the time invariant scheme shows gradual deterioration of the fraction of the covered area while the time varying algorithm maintains its initial coverage fraction.



(a) initial distribution



(b) deployment completed

Fig. 21. Initial deployment of the mobile nodes

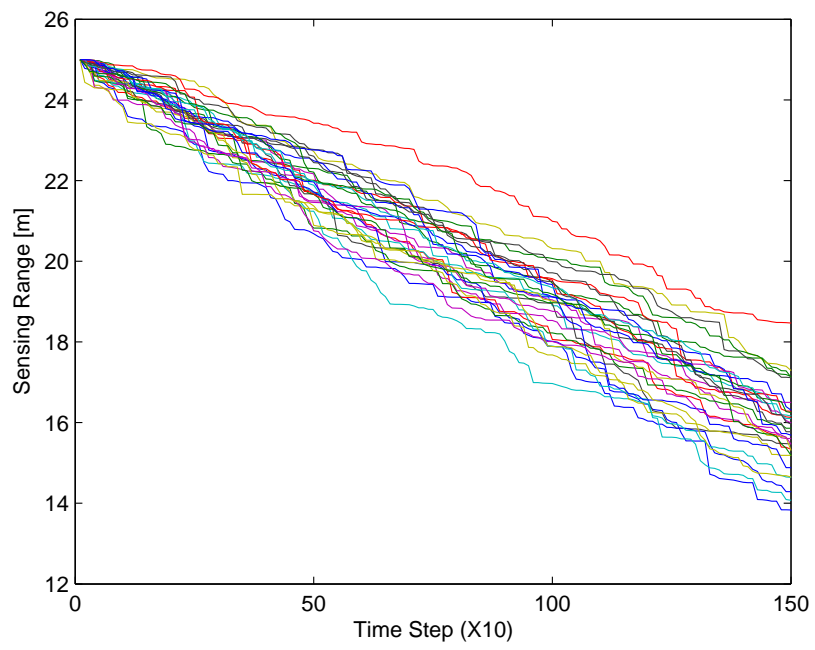
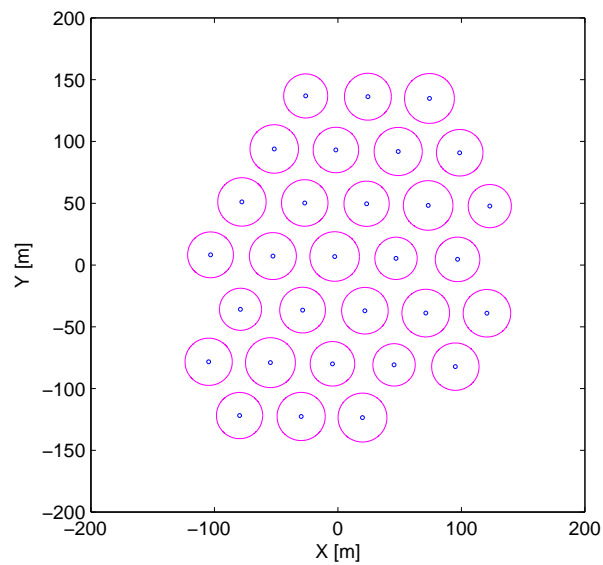
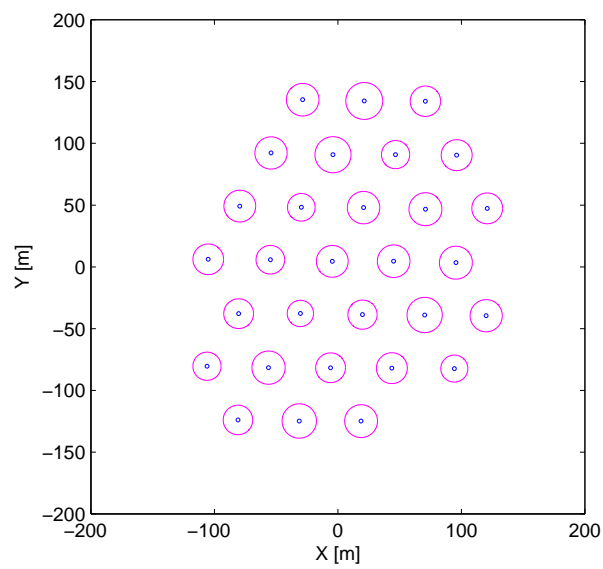


Fig. 22. Sensing range deterioration due to the power drainage

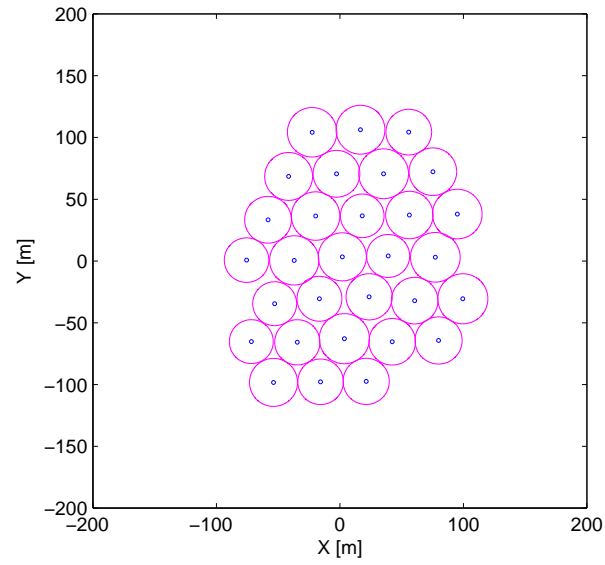


(a) stage 1

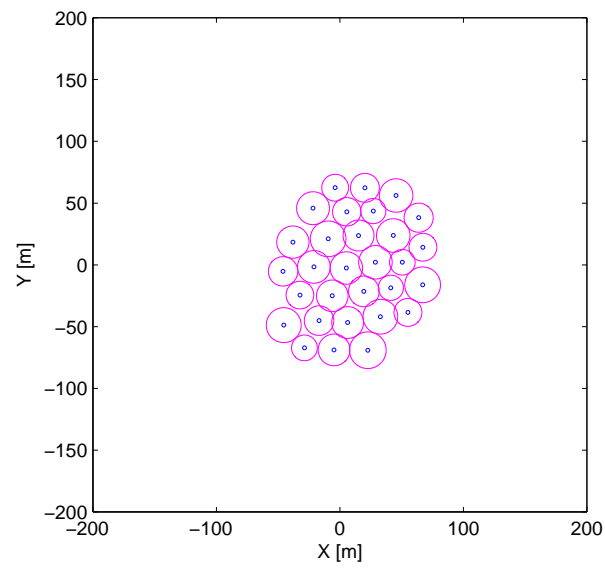


(b) stage 2

Fig. 23. Coverage maintenance with constant d



(a) stage 1



(b) stage 2

Fig. 24. Coverage maintenance with time varying d

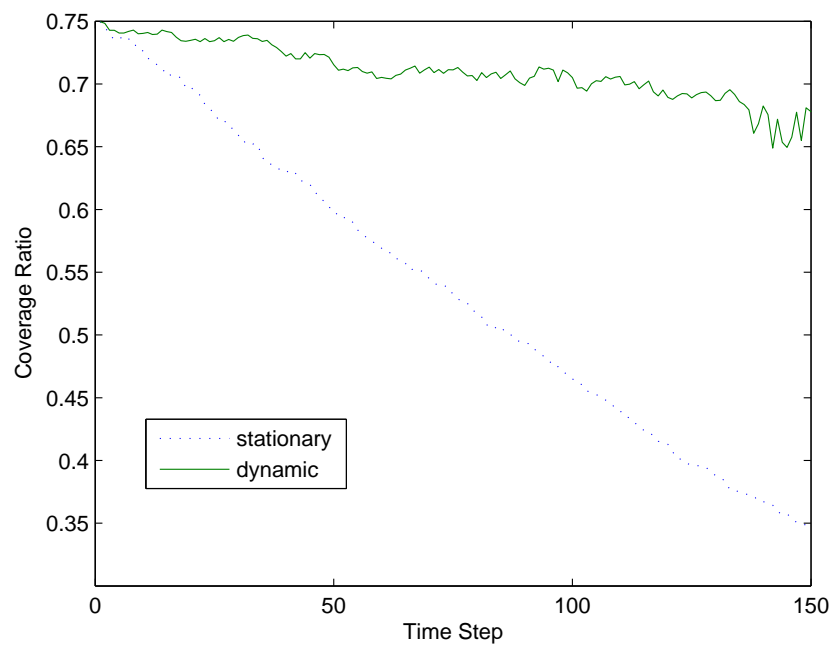


Fig. 25. Fraction of the covered area for two cases

CHAPTER VI

HARDWARE DEVELOPMENT

We have developed an autonomous mobile robot system to implement our algorithms. The robot is a 2-wheel, differential drive, intelligent robot, containing all of the basic components for autonomous sensing and navigation in a real-world environment. The devices include battery, drive motors, encoders and these devices are controlled via an onboard microcontroller.



Fig. 26. Mobile robot base: Rex-12 from Zagros Robotics

A. Mobile Base

The mobile base is a Rex-12 manufactured by Zagros Robotics (fig. 26). The base has 30 cm diameter round plastic deck on which various sensor suits can be mounted. It has two 15 cm diameter rubber wheels with two 7.5 cm castor wheels. This symmetric design of the drive wheels and castor wheels allows an in-place rotation as well as stable movement and high maneuverability. The drive wheels are differentially driven by reversible 12VDC

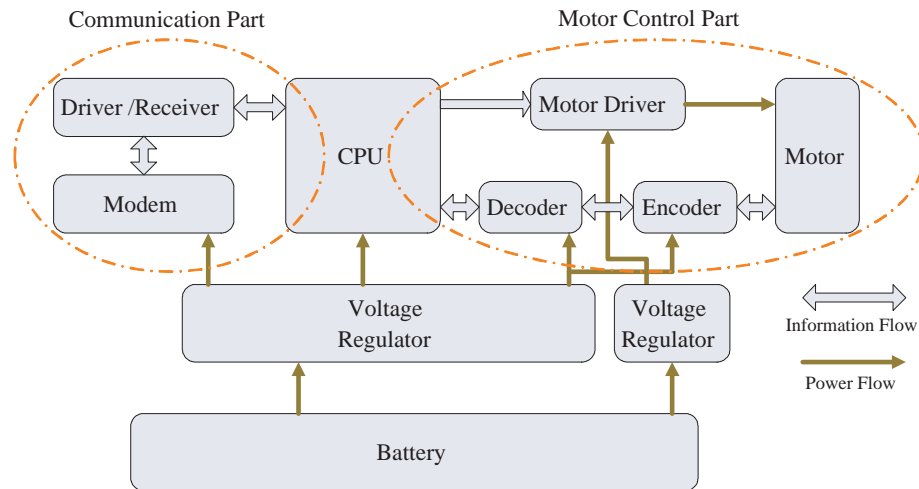


Fig. 27. System diagram for a mobile robot with power and information flows

motors. Each drive motor has a 500 pulse/rev HEDS 5500 optical quadrature shaft encoder which enables precise positioning, speed sensing and advanced dead-reckoning.

B. Mobile Robot Control System

System architecture of the control system is shown in fig. 27 and its major components are described in table I. All components are powered by a single 12V 2.2AH lead-acid rechargeable battery. Voltage regulator is to provide a regulated output voltage to the components. In this system, the regulator converts 12V to TTL/CMOS level 5V. The system consists of two major parts: motor control part and communication part.

C. Communication Part

1. Wireless module

Wireless communication unit is composed of two parts: MCB3100 which is a serial bluetooth wireless module, and MCR3210P which is a RS232 Interface board. Major specifications of MCB3100 is shown in table II, and its pin descriptions are illustrated in table

Table I. Components of a mobile robot for communication and motor control

Unit Name	Manufacturer	Component
CPU	Microchip	PIC 16F877
Motor Driver	Zagros Robotics	MC TI SN754410
Encoder	Agilent	HEDS5500
Decoder	Agilent	HCTL-2020
Voltage Regulator	STMicroelectronics	L7805
Driver/Receiver	Texas Instrument	MAX232
Modem	Dr Robot	MCB3100

Table II. Communication unit (MCB3100) specifications

	Specification
protocol	Bluetooth (class 2)
range	15m indoor, 45m outdoor
data rate	921.6/460.8/115.2 kbps
voltage consumption	3.3V

III. The MCR3210 module is a hardware matching interface compatible with standard RS232 electrical specifications. MCR3210 is capable of transmitting and receiving up to 1 M bits/sec with RTS/CTS handshaking. The physical connections between modules are shown in fig. 28. Hardware flow control (RTS/CTS) is used.

2. Voltage coverter

RS-232 port uses TIA/EIA-232-F voltage level while a microcontroller uses TTL level voltage. Max 232 is used to covert those different voltage levels. Max 232 has dual driver/receiver lines. Each driver converts the voltage level of a signal from a microcon-

Table III. Pin connection of MCB3100

Pin number	Name	Function
1	VCC	PIC 16F877
2	TXD	Data transmitting
3	RXD	Data receiving
4	CTS	Clear to send
5	RTS	Request to send
6	GND	Power supply ground
7	COMRST	Reserved
8	BTIN	Reserved

troller (TTL level) to the wireless modem (TIA/EIA-232-F level), while each receiver converts TIA/EIA level to TTL level. Typical pin connections of MAX 232 are shown in fig. 29.

D. Motor Control Part

1. Controller

Regulation and tracking of the given control input is implemented through a PD controller.

The control inputs (u_l, u_r) to the mobile robots are the linear wheel velocities, and are given

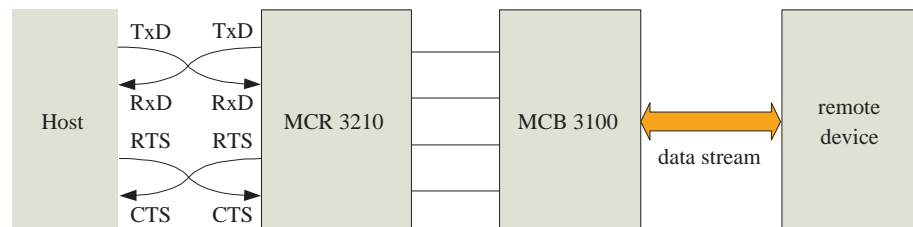


Fig. 28. Physical connection between the modules

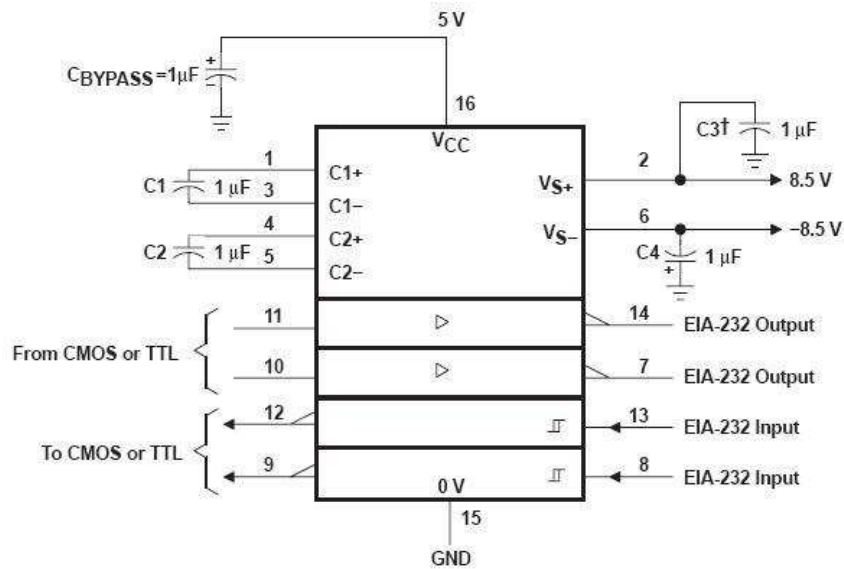


Fig. 29. Max232 pin connections

as

$$u_l = K_p e_l + K_d \dot{e}_l$$

$$u_r = K_p e_r + K_d \dot{e}_r$$

where K_p and K_d are proportional and derivative gains, respectively. e denotes error at the time step, and \dot{e} is its rate of change.

2. Interrupt

The frequency of the updating control law is determined by a interrupt routine provided by the micro controller. PIC16F877 has 14 interrupt sources, and timer based interrupts are used in this research. On PIC16F877, Timer 0 is an 8 bit timer/counter while Timer 1 and Timer 2 are 16 bit timer/counter. Timer 1 is used for the interrupt and timer 2 is reserved for PWM. Timer 1 register pair increments from 0x0000 to 0xffff and rolls over to 0x0000. The Timer 1 interrupt occurs on overflow.

Timer can be set to an arbitrary value using **setup_timer_1 (clock source|prescaler)**. The oscillator (crystal) source is either internal or external, and the prescaler determines the timer's resolution. Whatever the master oscillator frequency (F_{osc}) is, the internal (system) clock is always the oscillator frequency divided by 4. Therefore, the duration of one count (an overflow to next one) is given by

$$duration(sec.) = (number\ of\ ticks) * 4 * prescaler / F_{osc}$$

where the number of ticks in the timer 1 is 2^{16} as it is a 16 bit timer. We can modify the frequency of the interrupt using **set_timer1(value)**, where the timer begins at the *value*, and overflow occurs when it reaches 0xffff.

3. Motor speed control

Pulse Width Modulation (PWM) technique is used to control the motor speed. PWM regulates the output voltage by modulating its duty cycle, and the wheel speed is proportional to the output voltage. By switching voltage to the motor with the appropriate duty cycle, the output of PWM will approximate a voltage level at the desired velocity.

PIC16F877 microprocessor has 10-bit resolution PWM mode. Then the duty cycle (the amount of time the PWM signal is high) during each period is determined with a given 10 bit value as

$$ratio = value * (1/clock) * t2div \quad (6.1)$$

where clock is oscillator frequency and t2div is the timer 2 prescaler.

4. Mapping artificial force to a real robot

The dynamic system driven by the artificial potential is based on virtual interactions between the nodes. It means that the forces on the nodes are imaginary. This virtual force

will be mapped onto a real dynamic system composed of the real nodes. The mapping from virtual to real system is achieved by defining control laws which convert a virtual force to a velocity command.

Let us define u be a feedback control of the form

$$u = -\nabla V(\mathbf{r}),$$

where \mathbf{r} is the distance between the nodes. A discretized model is employed to implement control inputs to the system. Control inputs to a mobile base are velocities for wheels in case of wheeled vehicles. The change in velocity commands are approximated from the above equation as

$$\Delta \dot{\mathbf{x}} = (u - b\dot{\mathbf{x}})/m \cdot \Delta t,$$

where Δt is a sampling time. Then, a velocity command is given by $\dot{\mathbf{x}}(t_{i+1}) = \dot{\mathbf{x}}(t_i) + \Delta \dot{\mathbf{x}}$, where $t_{i+1} = t_i + \Delta t$. Note again, that $\Delta \dot{\mathbf{x}}$ and $\dot{\mathbf{x}}$ are bounded by physical system constraints. The maximum values are restricted to $|\dot{\mathbf{x}}| \leq v_{max}$ for the velocity, and $|\Delta \dot{\mathbf{x}}| \leq a_{max}$ for acceleration.

CHAPTER VII

CONCLUSIONS AND FUTURE WORK

A. Summary and Conclusions

We presented strategies for potential field based mobile sensor network deployment and maintenance. Potential field based artificial force algorithms provide a simple and efficient method to deploy large a number of sensors because the force is used as the control input for each node without any sophisticated control algorithms. Three key ideas that were dealt within this research are

- forming a hexagonal structure with artificial forces generated from potential fields
- developing a hierarchical structure for area coverage
- maintaining coverage using heterogeneous sensor model

With respect to coverage area, an hexagonal formation was shown to be the optimal placement when the same sensor model is used for all nodes. It also provides better uniformity that improves the system performance including load balancing and system life time. A force law inspired by gravitational force was employed to form such a hexagonal structure. Due to the nature of the proposed force law, the stability of the system was analyzed with discontinuous dynamics. A Lyapunov function which combines kinetic energy and potential energy was constructed and a nonsmooth version of Lyapunov stability theory and LaSalle's invariance principle were used to prove stability.

The main contribution of this proof is to expand the mutual relation between the force which is required to have a certain formation and the potential function which is used for the stability analysis. This is because the force is derived by taking the derivative of the potential. In other words, different formations can be achieved with different force laws.

The line integral which becomes the potential function is then taken to analyze the stability of the system. This procedure is the inverse of the conventional potential field methods, which first build potential functions and then use the derivative of the potential as a control input. Based on the proof given in this research, a stable system with a desired formation can be achieved.

Also developed was a deployment algorithm using a two layered hierarchical structure with upper and lower layers. A group of nodes formed a cluster which comprised of a head node and several member nodes. In forming such a cluster, the concept of active and passive nodes was introduced. An active node is influenced only by its neighboring active nodes, while a passive node is affected by both neighboring active nodes and passive nodes. Cluster heads are active nodes and member nodes are passive nodes. Upper layer of the hierarchical structure consists of active nodes and lower layer is composed of passive nodes. First, a cluster forms a hexagonal structure with given active and passive nodes concepts. Then active nodes establish communication links with neighboring active nodes, and they form a hexagonal structure at the upper level. While active nodes are moving to make such a hexagonal structure, a cluster takes rigid body motion in which passive nodes maintain the same distances and bearing angles with respect to an active node. Finally, after active nodes complete the formation, the hierarchical structure turns into a flat structure in which all nodes become identical.

The benefit of this scheme was shown in terms of uniformity. In the conventional incremental case, where nodes are initially placed in a small area and spread out using algorithms, the uniformity deteriorates as the number of nodes are increased. The hierarchical algorithm, meanwhile, was shown to be of almost constant uniformity. This improvement can be considered in two directions: one is to minimize the chances of being trapped in local minima, and the other is to reduce power consumption of the whole system. It had been shown that the system performance of the incremental algorithm is dependent on the

force model. As discussed in the beginning of this dissertation, potential based control laws induce the system to have locally minimized potential energy. Even though the force law was proposed to have a hexagonal structure, it had to be adjusted with the given number of nodes. In other words, global minimum is correlated with the value of α in the force law $F_{ij} = \alpha/r_{ij}^\beta$. The hierarchical structure reduces this troublesome tuning task by scattering the sensors in the wider area. The other virtue of the hierarchical structure in reducing total energy consumption is straightforward as it guarantees more balanced task distribution, and minimizes the communication load for each mobile node. Regardless of the initial deployment, a hierarchical structure was shown to be more efficient than a non-hierarchical structure.

Presented last was an autonomous maintenance algorithm for a mobile sensor network. To implement a more realistic sensor model, a stochastic sensor model was proposed to keep the desired detection reliability over the environment. The model reflects the decline of the sensor accuracy as the distance increases from the sensor. In addition, a time varying model was applied to represent sensor performance deterioration due to power decay. The power supplied by batteries is checked with a power alert system, and the power level is reflected so that the network maintains a desired detection reliability level. The scheme was compared with a time invariant sensor model, and the performance superiority to the time invariant model was shown by comparing the fraction covered by the network.

The main advantage of applying the described heterogeneous sensor model is to expand the potential field method not only for a regularized formation (ex. hexagonal structure) but also for an irregular arrangement of sensor nodes to achieve a certain criterion. In this research, the objective was to maintain the desired coverage performance. Various scenarios can be applied without changing the framework of this research.

B. Directions for Future Research

The deployment and coverage algorithms developed in this research used a potential field approach to achieve a desired performance. In connection with the natural drawbacks of the potential field approach, several directions for future research are outlined below.

The main weakness of the potential based schemes is that global optimization cannot be achieved. This is a fundamental weakness of the potential field based method, because only local interactions between the nodes are considered. Another major drawback of the scheme is the existence of local minima. In some cases, a local minimum induces an imperfect formation which reduces the uniformity if the objective is to achieve a hexagonal structure. These global optimization and local minima problems can be approached with the proposed hierarchical structure. Clusters are aggregated so that the overall shape of the network tends to be convex. The effect of the cluster size also needs to be determined.

Local minima can also cause collision among the mobile nodes if multiple nodes are lumped at a local minimum point. This phenomenon can be avoided if a potential function is taken so that the value around the node goes to infinity. However, as explained in this dissertation, such an approach is impractical because the force exerted on the neighboring node would be infinite as well, which is physically impossible due to the restrictions on the hardware. A low level controller which avoids collision with an emergency handler can be introduced and returns back to the original algorithm after avoiding the collision. Algorithms using computational geometry can be combined with a potential field method as long as it does not impair the distributed nature of the potential field based schemes. However, computational complexity has to be considered in this case.

Possible future directions include the development of power consumption models of the network and more sophisticated sensor models that incorporate sensor noise. Developed in this dissertation is an algorithm to maintain the coverage of the network. To predict the

system performance more precisely, a more detailed power consumption model is required. To be robust in the environment, sensor noise issues also need to be reflected in the system model.

REFERENCES

- [1] C. Chong, S. Jumar, "Sensor networks: Evolution, opportunities and challenges," *Proc. of the IEEE*, vol 91, no. 8, pp. 1247-1256, 2003.
- [2] G. Kantor, S. Singh, R. Peterson, D. Rus, A. Das, V. Kumar, G. Pereira, J. Spletzer, "Distributed search and rescue with robot and sensor teams," in *Proc. of the 4th Int'l Conf. on Field and Service Robotics*, Lake Yamanaka, Japan, 2003.
- [3] A. D. Chowdhury, S. Balu, "Consensus: a system study of monitoring applications for wireless sensor networks," in *Proc. of the IEEE Int'l Conf. on Local Computer Networks*, Tampa, FL, pp. 587 - 588, 2004.
- [4] J. O'Rourke, *Art Gallery Theorems and Algorithms*, New York: Oxford University Press, 1987.
- [5] S. Meguerdichian, F. Koushanfar, M. Potkonjak, M. Srivastava, "Coverage problems in wireless ad hoc sensor networks," in *Proc. IEEE INFOCOM Conf.*, Anchorage, AK, pp. 1380-1387, 2001.
- [6] D. W. Gage, "Command control for many-robot systems," in *the Nineteenth Annual AUVS Technical Symposium*, Huntsville, AL, 1992. Reprinted in *Unmanned Systems Magazine*, vol. 10, no. 4, pp 28-34, 1992.
- [7] O. Khatib, "Real-time obstacle avoidance for manipulators and mobile robots," *International Journal of Robotics Research*, vol. 5, no. 1, pp. 90-98, 1986.
- [8] P. Ogren, E. Fiorelli, N. E. Leonard, "Cooperative control of mobile sensor networks: Adaptive gradient climbing in a distributed environment." *IEEE Transactions on Automatic Control*, vol. 49, no. 8, pp. 1292-1302, Aug. 2004.

- [9] R. Bachmyer, N. E. Leonard. "Vehicle networks for a gradient descent in a sampled environment," in *Proc. of Conf. on Decision and Control*, Las Vegas, NV, pp. 112-117, 2002.
- [10] S. Poduri and G. Sukhatme, "Constrained coverage for mobile sensor network," in *Proc. of International Conference on Robotics and Automation*, New Orleans, LA, pp. 165-172, 2004.
- [11] D. O. Popa, C. Helm, H. E. Stephanou, A. Sanderson, "Robotic deployment of sensor networks using potential fields," in *Proc. of International Conference on Robotics and Automation*, New Orleans, LA, pp. 642-647, 2004.
- [12] J. Cortés, S. Martinez, T. Karatas, F. Bullo, "Coverage control for mobile sensing networks," *IEEE Transactions on Robotics and Automation*, vol. 20 no. 2, pp. 243-255, 2004.
- [13] Y. Zou and K. Chakrabarty, "Sensor deployment and target localization based on virtual forces," in *Proceedings of IEEE Conference on Computer Communications (INFOCOM)*, San Francisco, CA, pp. 1293-1303, 2003.
- [14] D. Shevitz, B. Paden, "Lyapunov stability theory of nonsmooth systems," *IEEE Trans. on Automatic Control*, vol. 49, no. 9, pp. 1910-1914, 1994.
- [15] M. Locatelli, U. Raber, "Packing equal circles in a square: a deterministic global optimization approach," *Discrete Applied Mathematics*, vol. 122, pp. 139-166, 2002.
- [16] P. G. Szabó, T. Csendes, L. G. Casado, I. García, "Packing equal circles in a square I. - problem setting and bounds for optimal solutions," in *New Trends in Equilibrium Systems*, Boston, MA: Kluwer Academic Publishers, pp. 1-15, 2000.

- [17] N. Heo, P. K. Varshney, "Energy-efficient deployment of intelligent mobile sensor networks," *IEEE Transactions on Systems, Man, and Cybernetics Part A: Systems and Humans*, vol. 35, no. 1, pp. 78-92, 2005.
- [18] H. Zhang, J. C. Hou, "Maintaining sensing coverage and connectivity in large sensor networks," *Ad Hoc & Sensor Wireless Networks*, vol. 1, pp. 89-124, 2005.
- [19] A. Filippov. *Differential Equations with Discontinuous Right-Hand Sides*, Dordrecht, the Netherlands: Kluwer Academic Publishers, 1988.
- [20] F. Clarke, *Optimization and Nonsmooth Analysis*, New York: Wiley, 1983.
- [21] J. Gao, L. J. Guibas, J. Hershberger, L. Zhang, A. Zhu, "Discrete mobile centers," *Discrete and Computational Geometry*, vol. 30, no. 1, pp. 45-65, 2003.
- [22] W. R. Heinzelman, A. Chandrakasan, H. Balakrishnan, "Energy-efficient communication protocol for wireless microsensor networks, in *Proc. of IEEE Hawaii Int'l Conf. Sys. Sci.*, Maui, HI, pp. 3005-3014, 2000.
- [23] J. Y. Yu and P. H. J. Chong, "A survey of clustering schemes for mobile ad hoc networks," *IEEE Communications Surveys*, vol. 7, no. 1, 2005.
- [24] A.D. Amis, R. Prakash, T. H. P. Vuong, D. Huynh, "Max-min D-cluster formation in wireless ad hoc networks," in *IEEE INFOCOM 2000*, Tel-Aviv, Israel, pp. 32-41, 2000.
- [25] M. Ma and Y. Yang, "Clustering and load balancing in hybrid sensor networks with mobile cluster heads," in *Proc. of Int'l Conf. Quality of Service in Heterogeneous Wired/Wireless Networks (QSHINE06)*, Waterloo, Canada, article no. 16, 2006.
- [26] K.-H. Tan, M. A. Lewis, "Virtual structures for high-precision cooperative mobile robotic control," *Autonomous Robots*, vol. 4, pp. 387-403, October 1997.

- [27] W. Ren, R. W. Beard, "Virtual structure based spacecraft formation control with formation feedback," in *AIAA Guidance, Navigation, and Control Conference*, paper no. AIAA-02-4963, 2002.
- [28] A. Howard, M. J. Mataric, G. S. Sukhatme. "An incremental self-deployment algorithm for mobile sensor networks," *Autonomous Robots*, vol. 13, no. 2, pp. 113-126, 2002.
- [29] S. Slijepcevic, M. Potkonjak, "Power efficient organization of wireless sensor networks," in *Proc. IEEE Int. Conf. Commun.*, vol. 2, pp. 472-476, 2001.
- [30] A. Elfes, "Occupancy grids: A stochastic spatial representation for active robot perception," in *Proc. 6th Conference on Uncertainty in AI*, Cambridge, MA, pp. 60-70, 1990.
- [31] V. Phipatanasuphorn and P. Ramanathan, "Vulnerability of sensor networks to unauthorized traversal and monitoring," *IEEE Transactions on Computers*, vol. 53, no. 3, pp. 364-369, Mar. 2004.

VITA

Jaeyong Lee

PERMANENT ADDRESS

Gyungnam Apt. # 5-405, Geoje3-Dong, Yeonje-Gu,
Busan, Korea

EDUCATION

Ph.D. in Mechanical Engineering, August 2007.

Texas A&M University

Advisor: Dr. Suhada Jayasuriya

M.S. in Mechanical Engineering, August 2002.

Texas A&M University

Advisor: Dr. Sooyong Lee

B.S. in Mechanical Engineering, February 2000.

Pusan National University, Busan, Korea

Advisor: Dr. Jae Weon Choi

The typist for this dissertation was Jaeyong Lee.